[17] T. Ishii, T. Yanagawa, T. Kawane, K. Yuki, J. Seita, H. Yoshida, S. Bannai, Murine peritoneal macrophages induce a novel 60-kDa protein with structural similarity to a tyrosine kinase p56^{lck}-associated protein in response to oxidative stress, Biochem. Biophys. Res. Commun. 226 (1996) 456–460.
[18] M. Okazaki, S. Ito, K. Kawakita, S. Takeshita, S. Kawai, F. Makishima, H. Oda, A. Kakinuma, Cloning, expression profile, and genomic organization of the mouse STAP/A170 gene, Genomics 60 (1999) 87–95.
[19] G.R. Beck Jr., B. Zerler, E. Moran, Gene array analysis of osteoblast differentiation, Cell Growth Differ. 12 (2001) 61–83.
[20] R.K. Vadlamudi, I. Joung, J.L. Strominger, J. Shin, p62, a phosphotyrosine-independent ligand of the SH2 domain of p56^{lck}, belongs to a new class of ubiquitin-binding proteins, J. Biol. Chem. 271 (1996) 20235–20237.
[21] A. Plus, S. Schmidt, F. Grawe, S. Stabel, Interaction of protein kinase C ζ with ZIP, a novel protein kinase C-binding protein, Proc. Natl. Acad. Sci. USA 94 (1997) 6191–6196.
[22] N. Laurin, J.P. Brown, J. Morissette, V. Raymond, Recurrent mutation of the gene encoding sequestsome 1 (SQST1/p62) in Paget disease of bone, Am. J. Hum. Genet. 70 (2002) 1582–1588.
[23] L.J. Hocking, G.J.A. Lucas, A. Daroszewska, J. Mangion, M. Olavesen, T. Cundy, G.C. Nicholson, L. Ward, S.T. Bennett, W. Wuyts, W.V. Hul, S.H. Ralston, Domain-specific mutations in sequestsome 1 (SQSTM1) cause familial and sporadic Paget's disease, Hum. Mol. Genet. 11 (2002) 2735–2739.
[24] F. Denizot, R. Lang, Rapid colorimetric assay for cell growth and survival: modifications to the tetrazolium dye procedure giving improved sensitivity and reliability, J. Immunol. Methods 89 (1986) 271–277.
[25] M.M. Monick, A.B. Carter, G.W. Hunninghake, Human alveolar macrophages are markedly deficient in REF-1 and AP-1 DNA binding activity, J. Biol. Chem. 274 (1999) 18075–18080.
[26] S.R. Carlsson, M. Fukuda, The lysosomal membrane glycoprotein Lamp-1 is transported to lysosomes by two alternative pathways, Arch. Biochem. Biophys. 296 (1992) 630–639.
[27] C.F. Harvey, C.H. Swartz, A.B.M. Badruzzaman, N. Keon-Blute, W. Yu, M.A. Ali, J. Jay, R. Beckie, V. Niedan, D. Brabander, P.M. Oates, K.N. Ashfaque, S. Islam, H.F. Hemond, M.F. Ahmed, Arsenic mobility and groundwater extraction in Bangladesh, Science 298 (2002) 1602–1606.
[28] M.G. Alam, G. Allison, F. Stagnitti, A. Tanaka, M. Westbrooke, Arsenic contamination in Bangladesh groundwater: a major environmental and social disaster, Int. J. Environ. Health Res. 12 (2002) 235–253.
[29] C.-H. Wang, J.-S. Jeng, P.-K. Yip, C.-L. Chen, L.-I. Hsu, Y.-M. Hsueh, H.-Y. Chiou, M.-M. Wu, C.-J. Chen, Biological gradient between long-term arsenic exposure and carotid atherosclerosis, Circulation 105 (2002) 1804–1809.
[30] K. Itoh, N. Wakabayashi, Y. Katoh, T. Ishii, T. O'Connor, M. Yamamoto, Keap1 regulates both cytoplasmic-nuclear shuttling and degradation of Nrf2 in response to electrophiles, Genes to Cells 8 (2003) 379–391.
[31] H.V. Aposhian, Biochemical toxicology of arsenic, in: E. Hodgson, J.R. Bend, R.M. Philpot (Eds.), Review in Biochemical Toxicology, vol. 10, Elsevier, Amsterdam, The Netherlands, 1989, pp. 265–299.
[32] M. Kwak, N. Wakabayashi, K. Itoh, H. Motohashi, M. Yamamoto, T.W. Kensler, Modulation of gene expression by cancer chemopreventive dithiolethiones through the Keap1–Nrf2 pathway: identification of novel gene clusters for cell survival, J. Biol. Chem. 278 (2003) 8135–8145.
[33] J. Shin, p62 and the sequestsome, a novel mechanism for protein metabolism, Arch. Pharm. Res. 21 (1998) 629–633.
[34] T. Geetha, M.W. Wooten, Structure and functional properties of the ubiquitin binding protein p62, FEBS Lett. 512 (2002) 19–24.

Identification of a novel Nrf2-regulated antioxidant response element (ARE) in the mouse NAD(P)H:quinone oxidoreductase 1 gene: reassessment of the ARE consensus sequence

Paul NIOI*, Michael McMAHON*, Ken ITOH†, Masayuki YAMAMOTO† and John D. HAYES*[1]

*Biomedical Research Centre, Ninewells Hospital and Medical School, University of Dundee, Dundee DD1 9SY, Scotland, U.K., and †Centre for Tsukuba Advanced Research Alliance and Institute of Basic Medical Sciences, University of Tsukuba, Tsukuba 305-8577, Japan

NQO1 [NAD(P)H:quinone oxidoreductase 1] has an integral role in cellular responses to oxidative stress. The expression of NQO1 is up-regulated in the mouse following challenge with electrophilic chemicals, in an Nrf2 (NF-E2 p45-related factor 2)-dependent fashion, but the molecular basis for this observation remains unexplained. Through characterization of the murine *nqo1* 5′-upstream region, we now show that Nrf2 regulates this gene directly via an ARE (antioxidant response element) that lies within a 24 bp region spanning nt −444 to −421. A comprehensive mutation study of this ARE revealed that it does not conform to the currently accepted ARE consensus sequence [(5′-TMAnnRTGAYnnnGCRwwww-3′, with essential nucleotides shown in capitals); two cytosine residues (shown in bold in the following sequence) that have been designated 'n' previously because they were thought to be redundant (5′-gagTcACaGTgA-GtCggCAaaatt-3′) have now been found to be essential for enhancer activity; two guanines (also shown in bold) previously regarded as essential for ARE function (5′-gagTcACaGTgA-GtCggCAaaatt-3′) have proven to be dispensable]. Examination of wild-type and *nrf2*$^{-/-}$ mouse embryonic fibroblasts demonstrated that Nrf2 is essential for both constitutive expression of NQO1 and its induction by sulphoraphane. Electrophoretic mobility-shift and chromatin immunoprecipitation assays revealed that Nrf2 associates, in low amounts, with the *nqo1* ARE under constitutive conditions, and following sulphoraphane challenge of cells, Nrf2 is recruited to the ARE in substantially greater quantities, as a heterodimer with the small Maf (musculoaponeurotic fibrosarcoma virus) protein, MafK. Also, MafK was found to bind the *nqo1* ARE in an Nrf2-independent fashion, and may contribute to transcriptional repression of the oxidoreductase gene. These findings allow a model for transcriptional control of *nqo1* through the ARE to be proposed. Furthermore, our results indicate that distinct AREs have differential sequence requirements, and a universally applicable consensus sequence cannot be derived.

Key words: antioxidant, antioxidant response element, Maf protein, Nrf2, oxidative stress, quinone reductase, sulphoraphane.

INTRODUCTION

Exposure of mammalian cells to electrophilic agents results in adaptive changes in gene expression designed to afford protection against similar insult. This is best characterized by the transcriptional activation of a 'battery' of genes encoding antioxidant and/or detoxication enzymes. The net consequence of this change in gene expression is an enhanced ability of the cell to conjugate and excrete reactive chemical species, coupled with an increased capacity to withstand oxidative stress [1]. Genes activated by such stimuli include those encoding the GST (glutathione S-transferase) isoenzymes, GCLC (glutamate cysteine ligase catalytic) and GCLM (glutamate cysteine ligase modulatory) subunits, HO-1 (haem oxygenase-1), ferritin and NQO1 [NAD(P)H:quinone oxidoreductase 1].

NQO1 is of particular interest, because in the mouse it is highly inducible by electrophiles and has key cytoprotective functions. It is a flavoprotein that catalyses the obligatory two-electron reduction of quinones, thereby inhibiting redox cycling of xenobiotics. This action is coupled with a central role in maintenance of two powerful endogenous antioxidants, α-tocopherol-hydroquinone and co-enzyme Q, in their reduced and active forms [2,3]. The importance of NQO1 has been further defined through germ-line mutagenesis studies. Mice lacking *nqo1* are substantially more susceptible to benzo[*a*]pyrene-induced skin carcinogenesis, and exhibit a marked increase in toxicity to menadione [4,5]. Furthermore, in humans, the *NQO1**2 allele (C609 → T) codes for an inactive and unstable form of NQO1, and individuals carrying this polymorphism show a greater incidence of certain cancers ([3], and references therein).

Evidence suggests that NQO1 plays an integral part in the cytoprotective response invoked during electrophilic insult. Using gene-knockout models, it has recently been demonstrated that the cap 'n' collar bZIP (basic leucine zipper) transcription factor Nrf2 (NF-E2 p45-related factor 2) is essential for the transcriptional activation of mouse *nqo1* and other cytoprotective genes following treatment with electrophilic cancer chemopreventive agents such as SUL (sulphoraphane), butylated hydroxyanisole and 1,2-dithiole-3-thione [6–11]. The molecular basis for the electrophilic induction of murine *nqo1* and the Nrf2-dependency of this phenomenon have not been reported.

A common feature of the promoter regions of genes that are induced by oxidative and electrophilic insult, in an Nrf2-dependent fashion, is the presence of a *cis*-acting sequence, the

Abbreviations used: ARE, antioxidant response element; bZIP, basic leucine zipper; ChIP, chromatin immunoprecipitation; EMSA, electrophoretic mobility-shift assay; GST, glutathione S-transferase; GCLC, glutamate cysteine ligase catalytic; GCLM, glutamate cysteine ligase modulatory; HGMP, Human Genome Mapping Project; LDH, lactate dehydrogenase; Maf, musculoaponeurotic fibrosarcoma virus; MEF, mouse embryonic fibroblast; NQO1, NAD(P)H:quinone oxidoreductase 1; Nrf2, NF-E2 p45-related factor 2; PAC, P1 artificial chromosome; RACE, rapid amplification of cDNA ends; SUL, sulphoraphane.

[1] To whom correspondence should be addressed (e-mail john.hayes@cancer.org.uk).

ARE (antioxidant response element). AREs have been identified in genes including mouse *gsta1*, *ho-1* and Ferritin H [12–14], rat *GSTA2* and *NQO1* [15,16], and human *NQO1* and *GCLC* [17,18]. The ARE appears to confer a general transcriptional sensitivity to induction by compounds capable of generating oxidative stress within the cell [19]. The 'core' ARE consensus sequence was originally defined, by mutational analysis of the rat *GSTA2* enhancer and comparison with the rat *NQO1*ARE, as comprising the sequence 5′-RGTGACnnnGC-3′ (where 'n' is used to denote residues considered to be redundant) [20]. Subsequent work suggested that the ARE is better represented by an extended sequence, 5′-TMAnn**RTGAYnnnGC**Rwwww-3′, where the 'core' is highlighted in bold [21].

Oxidative stress results in the nuclear accumulation of Nrf2 [22–26]. Gel-shift assays have shown that Nrf2 can bind ARE sequences *in vitro* as a heterodimer with other bZIP factors, such as small Maf (musculoaponeurotic fibrosarcoma virus) proteins, and it is thereby hypothesized to direct gene expression [7]. Curiously, overexpression of small Maf proteins, e.g. MafK, is generally associated with repression of ARE-driven transcription [27–29].

The above findings infer that *nqo1* transcription may be under the control of an ARE that is regulated by Nrf2. However, the 5′-upstream region of the mouse *nqo1* gene has not been reported, and it is not known precisely how Nrf2 influences expression of the oxidoreductase gene. In the present study, the 5′-upstream region of murine *nqo1* has been cloned, and here we identify a novel ARE that controls both constitutive and inducible gene expression. A systematic mutational study of this element has been undertaken that has highlighted significant differences in sequence requirements of distinct AREs, and demonstrated shortcomings in the predictive value of the consensus sequence. Nucleotides within the 'core' ARE that were previously thought to be degenerate are shown in this study to be fundamental to the function of the element, and other bases regarded as essential for its function were found to be dispensable. Evidence is presented from analysis of *nrf2*$^{-/-}$ MEFs (mouse embryonic fibroblasts), showing that Nrf2 is vital for constitutive and SUL-inducible expression of NQO1. Nrf2 associates with the *nqo1* ARE under constitutive conditions, and is recruited further, in markedly higher amounts, as a heterodimer with MafK, following exposure of cells to SUL. Interestingly, MafK was also found to bind the *nqo1* ARE in an Nrf2-independent fashion, and it may be a central regulator of this enhancer required for both transcriptional activation and repression.

MATERIALS AND METHODS

Chemicals and reagents

All chemicals were of the highest quality grade, and were supplied, unless otherwise stated, either by Sigma–Aldrich Company Ltd, or by BDH Laboratory supplies. SUL (> 98 % pure) was obtained from LKT Laboratories. Dimethyl pimelimidate was from Pierce. Amersham Biosciences UK Ltd supplied all radioactive isotopes used. Formaldehyde was purchased from Fisher Scientific Ltd. Oligonucleotides were purchased from MWG Biotech AG. Probes for TaqMan® chemistry, labelled with a 5′ fluorescent reporter dye (6-carboxyfluorescein phosphoramidite) and a 3′ quenching dye (6-carboxy-tetramethyl-rhodamine), were synthesized by Cruachem Ltd. Trizol® reagent and all media supplements for cell culture were purchased from Life Technologies Inc. Ltd. Unless stated otherwise, all antibodies used were purchased from Santa Cruz.

Cell culture

Mouse hepatoma Hepa-1c1c7 cells (European Collection of Animal Cell Cultures) were maintained in minimum essential Eagle's medium, with the Alpha modification (Sigma) supplemented with 10 % (v/v) heat-inactivated fetal bovine serum, 50 units/ml penicillin/streptomycin mix and 2 mM L-glutamine. Rat liver RL-34 cells (Japanese Cancer Research Resources Bank) were grown in Dulbecco's modified Eagle's medium (Life Technologies Inc. Ltd) supplemented as described above. Wild-type and Nrf2-null MEFs were prepared from *nrf2*$^{+/+}$ and *nrf2*$^{-/-}$ mouse lines respectively [7], by the method of Tiemann and Deppert [30]. MEF cells were maintained in BIOCOAT™ collagen-coated flasks (Becton Dickinson Labware), and grown in medium supplemented with 10 ng/ml human recombinant epidermal growth factor, 1 × insulin transferrin selenium and 10 % (v/v) fetal bovine serum. All cell lines were maintained at 37 °C and 5 % CO_2.

It was established by using the MTT cytotoxicity test [31] that the doses of SUL used to treat Hepa-1c1c7, RL-34 and MEF cells did not affect their viability.

Plasmids

The 5′-upstream region of *nqo1* was amplified by PCR using the oligonucleotides, 5′-CGCCTCGAGGCCTCTGAATACTTTCAACAA-3′ and 5′-GCGAAGCTTTCGGAGAGATCCTTAGGGCTG-3′ and cloned into the pGL3-Basic (Promega) luciferase reporter vector to create −1016/*nqo5′-luc*. A mammalian expression vector for murine Nrf2 was generated by PCR amplification of the mouse cDNA using the oligonucleotides, 5′-ATGATGGACTTGGGAGTTGCCACCGCCAGGACTAC-3′ and 5′-TCACGTAGAATCGAGACCGAGGAGAAGGGTTAGG-3′ and the resulting product was cloned into pcDNA4/HisMax© (Life Technologies Inc. Ltd). cDNAs encoding Nrf2, MafK and MafG were cloned into the *NdeI/XhoI*, *NdeI/Eco*RI and *NdeI/Bam*HI sites respectively of pET15b (Novagen) for subsequent bacterial expression. The primer pairs used were: Nrf2, 5′-CCGCCCTCCATATGATGGACTTGGA-3′ and 5′-CTAAGAAATTAACTCGAGAGTTAAA-3′; MafK, 5′-AGGGCCCGGCATATGACGACTAATC-3′ and 5′-TGTGCCAGGGATCCTGGGATAGGCA-3′; MafG, 5′-CATATGACGACCCCCAATAAAGGAA-3′ and 5′-GAGCTCAAAGACCTGCCTGGCAACT-3′; underlined bases are mismatches to incorporate restriction sites. Single-point mutant ARE constructs were made by annealing complementary 47 bp oligonucleotides (representing nt −454 to −414) with overhangs that allowed ligation of double-stranded DNA into the pGL3-Promoter (Promega) luciferase reporter vector.

Site-directed mutagenesis

Mutations were introduced into the ARE in the 5′-upstream region of *nqo1* using the GeneEditor kit (Promega), according to the manufacturer's instructions. Oligonucleotides used contained the mutated nucleotides, shown below flanked on either side by 18–24 bp of wild-type sequence.

Probing of mouse genomic PAC (P1 artificial chromosome) filters

A gridded murine genomic PAC library RPCI-21 [32] was supplied by the UK HGMP (Human Genome Mapping Project) Resource Centre (Babraham, Cambridge, U.K.) on seven filters. Screening was carried out using rat NQO1 cDNA [33] randomly primed using the Prime-It® II labelling kit (Stratagene).

Hybridization and washing were carried out at 68 °C as instructed by the library manufacturer (http://www.chori.org/bacpac/). Following a 48 h exposure to autoradiographic film, positive clones were identified by the position and orientation of duplicated spots on the gridded filters, and upon request were supplied by the HGMP Resource Centre. Clone identity was confirmed by Southern blotting and PCR using the exon–intron boundary information reported previously [5].

Genome walking and 5′ RACE (rapid amplification of cDNA ends)

The TOPO® Walker kit (Life Technologies Inc. Ltd) was used to isolate the 5′-upstream region of *nqo1* from the genomic clone, 528 J08, isolated from the PAC library RPCI-21, as described in the manufacturer's protocol. Gene-specific primers used were 5′-ATGGCTCGAGATGTTGAGGGA-3′ (GSP1) and 5′-TCGGAGAGATCCTTAGGGCTGGCT-3′ (GSP2). The resulting product was cloned into pCR®Blunt (Life Technologies Inc. Ltd) and sequenced; this was conducted on three separate occasions. Subsequent PCR reactions, using genomic DNA as template, confirmed the results.

The transcriptional start site of *nqo1* was determined with the SMART™ RACE cDNA Amplification Kit (Clontech) according to the manufacturer's instructions using total RNA isolated from Hepa-1c1c7 cells. The gene-specific primer used was 5′-GTGATGGCCCACAGAGAGGCCAAA-3′. Reaction products were cloned into pCR4-TOPO® (Life Technologies Inc. Ltd) and sequenced. Ten separate clones were analysed.

DNA transfection and luciferase reporter gene assays

Cells were transfected at 70 % confluence using Lipofectin® Reagent (Life Technologies Inc. Ltd), according to the manufacturer's guidelines. In all transfections the pRL-TK *Renilla* reporter vector (Promega) was used as an internal control. Cells were treated 16 h post-transfection with 5 μM SUL or vehicle [0.1 % (v/v) DMSO] for a total of 24 h. Cells were lysed and *Renilla* and firefly luciferase activities were measured using the Dual-Luciferase® Reporter Assay System (Promega) and a Turner Designs TD-20/20 luminometer. Luciferase activities were normalized to *Renilla* internal control luminescence.

Preparation of nuclear extracts and immunodepletion

RL-34 or Hepa-1c1c7 cells were allowed to grow to 70 % confluence before being treated with either 5 μM SUL or vehicle [0.1 % (v/v) DMSO] for 4 h. Nuclear extracts were subsequently made using the NE-PER™ kit (Pierce) and stored at − 80 °C until required. Immunodepletion of nuclear extracts was performed using control rabbit IgG, anti-Nrf2 or anti-MafK antibodies in combination with Dynabeads® Protein G (Dynal Biotech), according to the supplied protocol. Briefly, 8 μg of IgG at a concentration of 200 μg/ml was added to 20 μl of washed Dynabeads Protein G and incubated at 4 °C for 30 min with rotation. Beads were washed twice with PBS, and then twice with 0.2 M TEA (triethanolamine), pH 8.2, before being incubated for 30 min at 20 °C in 20 mM dimethyl pimelimidate dissolved in 0.2 M TEA, pH 8.2. Following further incubation for 15 min in 50 mM Tris/HCl, pH 7.5, beads were washed three times in PBS containing 0.1 % (v/v) Tween-20. Thereafter, nuclear extract (80 μg of protein) was added to the beads and incubated at 4 °C for 30 min, before being transferred to a fresh batch of IgG-coupled beads and left for a further 1 h at 4 °C. Extracts depleted of Nrf2 or MafK were used immediately in downstream applications, or were flash-frozen in liquid nitrogen and stored at − 80 °C until required.

Production of purified Nrf2 and small Maf proteins

pET15b plasmids containing the cDNAs for Nrf2, MafG or MafK were expressed in *Escherichia coli* BL21 CodonPlus (DE3) RIL cells (Novagen) as His_6-tagged proteins, and purified using standard methods.

EMSA (electrophoretic mobility-shift assay)

EMSA reactions were conducted in 20 mM Hepes, pH 7.9, containing 1 mM EDTA, 50 mM KCl, 5 mM $MgCl_2$, 4 % (v/v) glycerol, 1 mM dithiothreitol, 3 μg/ml poly(dI-dC), 47-bp internally labelled *nqo1* ARE (1×10^4 c.p.m.) and either 7.5 μg of protein from nuclear extracts/immunodepleted extracts or 50 ng of each recombinant bZIP protein. In competition experiments, a 20-, 50- or 100-fold molar excess of unlabelled wild-type or mutant ARE was also included in the reaction. Reactions were incubated for 20 min at 20 °C before being subjected to electrophoresis under native conditions through a 4.5 % (w/v) polyacrylamide gel in 0.5 × TBE buffer at 4 °C. Gels were fixed [in an aqueous solution containing 20 % (v/v) methanol and 10 % (v/v) acetic acid], dried and exposed to autoradiographic film for 16 h at − 70 °C.

RNA isolation and semi-quantitative real-time PCR (TaqMan®)

Total cellular RNA was isolated from cell lines using Trizol® reagent according to the supplied guidelines. Single-stranded cDNA was synthesized as described previously [6]. *TaqMan*® analyses were performed on the PerkinElmer/Applied Biosystems Prism Model 7700 Sequence Detector instrument. For measurement of cDNA corresponding to mouse *nqo1* mRNA, the forward primer was 5′-GCAGGATTTGCCTACACAATATGC-3′, the reverse primer was 5′-AGTGGTGATAGAAAGCAAGGTCTTC-3′, and the probe was 5′-CCATGTACGACAACGGTCCTTTCCAGAA-3′. For measurement of cDNA corresponding to rat NQO1 mRNA, the forward primer was 5′-GCAGGATTCGCCTACACGTATG-3′, the reverse primer was 5′-GGTGATGGAAAGCAAGGTCTTC-3′, and the probe was 5′-CACCATGTATGACCAAGGTCCTTTCCAGAATA-3′. In both mouse and rat samples the level of 18 S rRNA was used as an internal standard.

SDS/PAGE and Western blotting

Western blotting for NQO1, Nrf2 and MafK proteins was performed as described previously [33]. Antiserum against rat NQO1 was available from a previous study [33].

ChIP (chromatin immunoprecipitation) assays

These were conducted essentially as described previously [34]. Immunoprecipitations were performed using control rabbit IgG, anti-Nrf2 or anti-MafK antibodies. Immunoprecipitated material or 3 μl of 1:100 dilution of input was used for 35 cycles of PCR with the following primers: the *nqo1* ARE, 5′-GCAGTTTCTAAGAGCAGAACG-3′ and 5′-GTAGATTAGTCCTCACTCAGCCG-3′ (186 bp); the *ldh* promoter region, 5′-GCAAAGCCAGTACTCTTTCTG-3′ and 5′-CGGCCATGTTCTGAATCCAAG-3′ (163 bp).

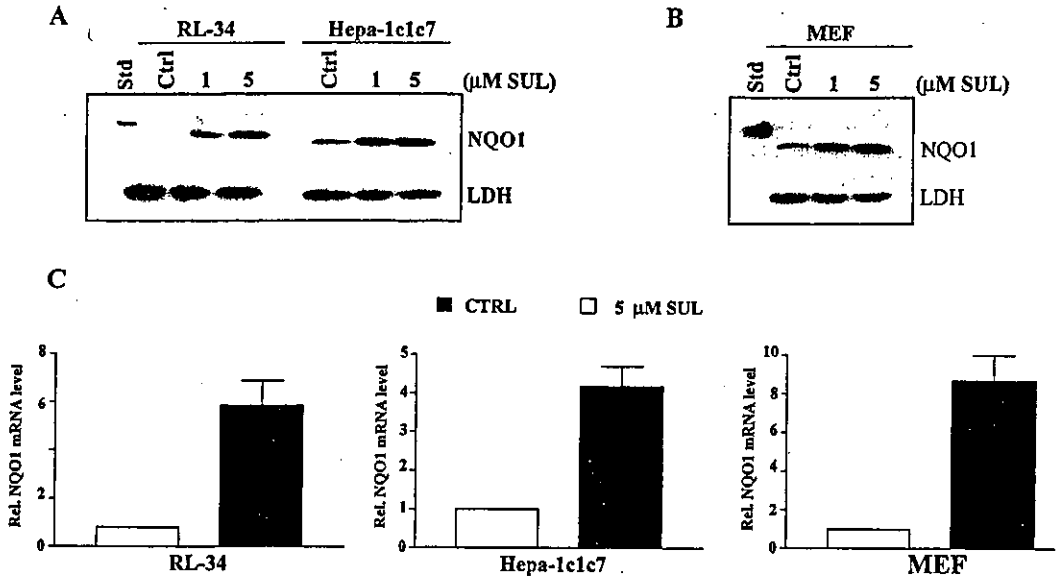

Figure 1 NQO1 protein and mRNA are inducible in RL-34, Hepa-1c1c7 and MEF cells

(A and B) Western blot analysis of NQO1 protein levels. Cell lines (as indicated) were treated for 24 h with either the stated dose of SUL or vehicle [0.1 % (v/v) DMSO; 'Ctrl']. Following lysis, 10 μg of total cellular protein was resolved by SDS/PAGE and blotted with NQO1 or LDH antibodies. A His_6-tagged rat NQO1 standard (Std) is shown on each gel. (**C**) TaqMan® analyses of NQO1 mRNA levels. Cell lines (as indicated) were treated for 24 h with 5 μM SUL or vehicle [0.1 % (v/v) DMSO; 'CTRL']. Following isolation of total RNA and reverse transcription, real-time PCR was conducted. Values from vehicle-treated cells were arbitrarily set to 1.0 in each case and all other results expressed relative to this. Values are means ± S.D. from three separate experiments.

Statistical analyses

This was determined using a one-way analysis of variance with 99 % confidence intervals and a Newman–Keuls post-test.

RESULTS

NQO1 protein and mRNA are induced by SUL treatment of rodent liver and embryonic fibroblast cell lines

SUL is a potent stimulator of detoxication enzyme expression [35]. The presence of an ARE within a gene promoter confers sensitivity to induction of transcription by SUL. Previous reports have regarded mouse *nqo1* as a potential ARE-bearing gene by virtue of its inducibility by electrophilic chemicals [8]. To assess this possibility further, the response of the oxidoreductase to SUL was examined in Hepa-1c1c7 and MEF cells. The rat RL-34 cell line was also studied, as a positive control, since an ARE has been described in rat NQO1 [16].

Western blotting showed that exposure of Hepa-1c1c7, MEF and RL-34 cells to SUL leads to a significant increase in NQO1 protein (Figures 1A and 1B). *TaqMan*® chemistry revealed this induction was reflected at the mRNA level, with Hepa-1c1c7, MEF and RL-34 cells showing increases of around 4-, 9- and 7-fold respectively (Figure 1C).

The 5′-upstream region of mouse *nqo1* contains a functional ARE

The above findings indicate that mouse *nqo1* contains an ARE. To evaluate this possibility, a genomic *nqo1* clone (528 J08) was isolated from PAC gridded filters. An approx. 1.0 kb portion of the 5′-upstream region was obtained by genome walking, and was sequenced (Figure 2). The transcriptional start site of *nqo1* was elucidated by SMART™ RACE, and was found to lie 22 bp downstream from a putative TATA box and 129 nt upstream from the ATG initiation codon.

```
                                                    CTTTTAATGATGGCAATCTGTTATAA
                                                    -1016
TGTCTACCCTACTTTGGGAGCTTGACCAAGGCACACACATACATGTAGGGTCTTTATT
-990
CCAACCCTTTTTCTTTCTTTCTCTGTTTTTGAGACAGGGTCTCACCTATGTAGCCCTG
-932
GCTGTTGTTCTAGCACTAGCTATGTGGACCAGTCTGGCCTTAAACTCAGAGATCTGCC
-874
TGCTTCTGGCACCCAAGTGATGGGATTAAAAGCATGTACTAGTCGTGGTGGCGCACTC
-816
CTTTAATCCCAGCACTTGGGAGGCAGAGTGCAGGTGGATTTCTGAGCTTCGAGGCCAG
-758
CCTGGTCTACAGAGTGAGTTCCAGGACAGCCAGGGCTACACAGAGAAACACTTCCCTG
-700
TGGCTGCTGTCTCCTGCCAGCTTTGCTCTGGCTTCCTAGAGAGTCGCACAGATGAGTT
-642
CCCCGTTACCTGGTCACCGGGGGCAAAGTTGAGGAGACCCAAGTGTGTATACCCAGGG
-584
AGCAGTTTTTGCAGTTTCTAAGAGCAGAACGCAGCACGAATTCATTTCACACGAGGAC
-526
AAGTCTCTCTGAACTTTCAGTCTAGAGTCACAGTGAGTCGGCAAAATTTGAGCCCATC
-468                          -441  ARE-related  -421
CGTTTTGCTGCCCCACCCTTCCCCTAGCGTGCAAAGGTGACTTCCCACGGCTGAGTGA
-410
GGACTAATCTACACAGGCTGATTATGTAGGCAGGTCCCACGAAGCTCGAAAAATTCTG
-352
TTGGAAATTTCCATTTTGTACCCAGGAGGTCTTGGGACAGGGAGCAGATGAATTTATT
-294
CAATATGTCCCCATATCCTCAAATTCTCTCTCACTCCCTTGCTCCCGGGGAACCCTTT
-236
TGACTTCCATATACAGGAGTCCTAGTCCAGCCCCAAACTGCTTCTCCCTGCCAAAAAC
-178
TTGGTATCTTCCCAAGATGCCTCTGGGTTCTGGAGTCCAGCCCCGCCCTCGCTGGCTG
-120
CTCTGCACAGTGGGCTGGGCGGGCATAAGCAGGATATAAAGCCTTCGCTCAGCCCATA
-62                                  TATA-Box
CCCCaaggctcagctcttactagcctagcctgtagccagccctaaggatctctccga
-4  ↳
    +1
```

Figure 2 Nucleotide sequence of the 5′-upstream region of mouse *nqo1*

The nucleotide sequence of the first 1016 bp of the mouse *nqo1* 5′-upstream region is shown. The transcriptional start site is indicated by +1 and a probable TATA box is underlined. The position of the putative ARE (nt − 421 to − 441) is indicated.

A region bearing significant similarity to the rat *NQO1* ARE [16,36] was found to be located between nt −441 and −421 of mouse *nqo1* (Figure 2). This is related to, but does not obey the rules of, the current ARE consensus sequence [20,21]. To assess whether the putative *nqo1* ARE is functional, a luciferase reporter construct driven by the promoter of this gene was generated (−1016/*nqo5′–luc*). Following transient transfection with this construct, treatment of either RL-34 or Hepa-1c1c7 cells with SUL led to 9.6- and 3.4-fold increases in luciferase activity respectively (Figures 3B and 3C). Site-directed mutagenesis was used to introduce mutations across a 36 bp region encompassing the putative ARE, along with sequence flanking this element (Figure 3A, Mut 1). These alterations not only abolished the SUL-responsiveness of the construct, but also produced a >80% decrease in constitutive luciferase activity when compared with wild-type −1016/*nqo5′–luc* (Figures 3B and 3C). Mouse *nqo1* therefore contains a functional ARE that regulates both constitutive and inducible gene expression.

In order to delineate further the *nqo1* ARE, a series of smaller mutations were generated; nucleotides encompassed by Mut1 (−450 to −415) were divided into five 'blocks', each of which was mutated individually (Figure 3A, Mut2 to Mut6). Mutations within the most-5′ and -3′ 'blocks' (Mut2 and Mut6 respectively) had no functional impact upon the promoter (Figures 3B and 3C), indicating that the enhancer is contained between these regions. Consistent with this conclusion, the three block mutations flanked by Mut2 and Mut6 (Figure 3A, Mut3, Mut4 and Mut5) all affected the function of the construct in a similar manner to Mut1 (Figures 3B and 3C). These results clearly demonstrate that the mouse *nqo1* ARE lies within a 24 bp region spanning bp −444 to −421.

Mutation of individual nucleotides within the *nqo1* ARE influences enhancer function

It has been proposed, on the basis of limited mutagenesis information and multiple-sequence alignments, that rules can be defined to dictate the permutations of nucleotides permitted in each position of an ARE [21]. According to this hypothesis, base requirements in certain positions are flexible, with any nucleotide being tolerable, whereas stringent requirements exist elsewhere, with only one base being acceptable. In order to analyse the importance of individual bases in mouse *nqo1* ARE function, and therefore test the aforementioned consensus sequence, a comprehensive series of ARE–luciferase reporter constructs were made. Every base lying between, and including, positions −444 to −421 of *nqo1* was mutated individually to create the most severe alteration possible; purines were converted to pyrimidines, and vice versa. RL-34 cells were transiently transfected with these mutant constructs, and luciferase activity was measured following treatment with either vehicle or SUL. The majority of alterations resulted in a decrease in the absolute level of luciferase activity in SUL-treated cells when compared with that observed for the wild-type ARE (Figure 4). However, many of the constructs, while not giving wild-type levels of responsiveness, still constituted functional AREs. There were, nevertheless, several mutations that rendered the element completely unreactive to SUL. Alteration of nucleotides shown in capital letters in the sequence, 5′-gagTcACaGTgAGtCggCAaaatt-3′, resulted in plasmids in which no significant difference was observed between luciferase activities from vehicle and SUL-treated transfectants (Figure 4). These bases are the most critical for *nqo1* ARE function, and may provide important contact points for transcriptional regulators.

It is noteworthy that a G → T substitution (shown underlined) in position 9 of the *nqo1* ARE, (5′-GAGTCACATTGAGTCGG-CAAAATT-3′), led to a substantial increase (>15-fold) in constitutive luciferase activity, although induction by SUL was lost (Figure 4). Given that this mutation renders the construct unresponsive to SUL, it is considered to represent a deleterious loss of regulation and is unacceptable for ARE function. Further EMSA experiments indicated this alteration created a binding site for a transcription factor that does not bind the wild-type sequence (results not presented).

A

```
WT:   AGTCTA GAGTCACA GTGAGTCGGC AAAATT TGAGCC
Mut1: GGGCGA TAATTAGA GATACTAGAC CACGTC CGGACA
Mut2: GGGCGA GAGTCACA GTGAGTCGGC AAAATT TGAGCC
Mut3: AGTCTA TAATTAGA GTGAGTCGGC AAAATT TGAGCC
Mut4: AGTCTA GAGTCACA GATACTAGAC AAAATT TGAGCC
Mut5: AGTCTA GAGTCACA GTGAGTCGGC CACGTC TGAGCC
Mut6: AGTCTA GAGTCACA GTGAGTCGGC AAAATT CGGACA
```

B

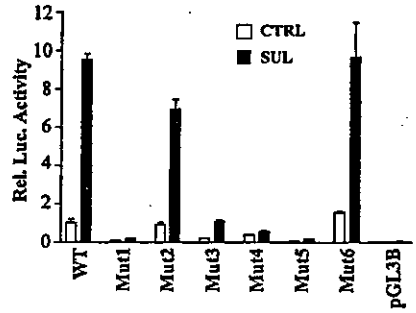

C

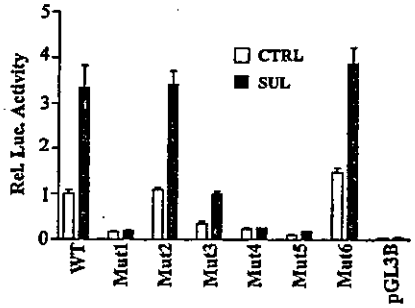

Figure 3 Mutational analysis of the *nqo1* ARE

(**A**) Wild-type and mutant ARE sequences. The 1.0 kb fragment of the *nqo1* 5′-upstream/flanking region, as shown in Figure 2, was cloned into the pGL3-Basic luciferase reporter vector to create the recombinant plasmid −1016/*nqo5′–luc*. The sequence of the ARE region of this construct is shown (WT). Mutations were introduced within this ARE region to create the mutant constructs Mut1 to Mut6. Mutated nucleotides are underlined in each case. The region showing similarity to the rat *NQO1* ARE and ARE-consensus sequence is shown in bold. (**B** and **C**) RL-34 and Hepa-1c1c7 cells, respectively, were transfected with 1 μg of wild-type or mutant ARE reporter constructs, as indicated. pGL3B represents reporter vector containing no insert. Following transfection (18 h), cells were treated with 5 μM SUL or vehicle [0.1% (v/v) DMSO; 'CTRL'] for 24 h. Cells were lysed and luciferase reporter assays were conducted. Values for vehicle-treated cells transfected with the −1016/*nqo5′–luc* reporter construct were arbitrarily set to 1.0, and all other results were expressed relative to this. All results were normalized to *Renilla* luciferase internal control luminescence. Results are shown as means ± S.D. for three separate experiments.

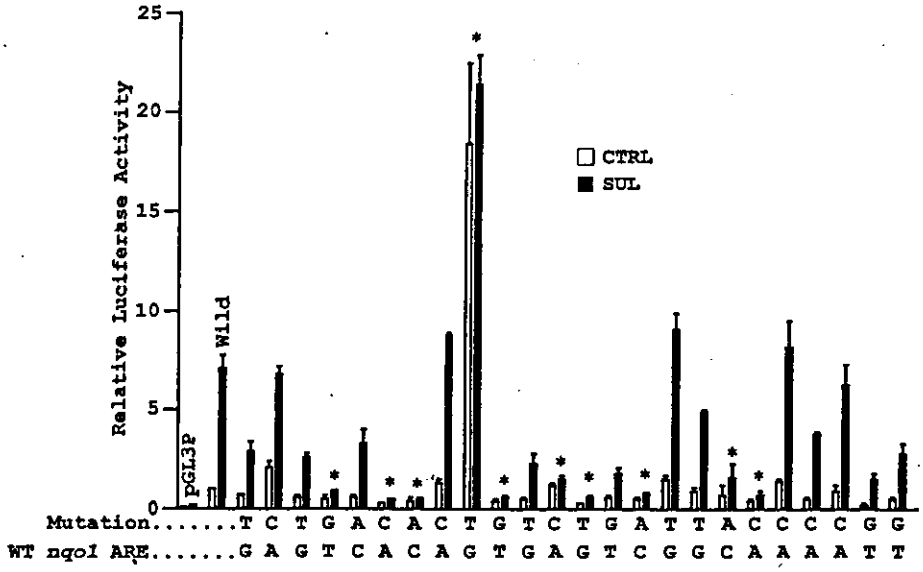

Figure 4 Single-point mutational analysis of the *nqo1* ARE

Oligonucleotides corresponding to the *nqo1* ARE sequence (−454 to −414), or mutants thereof, were cloned into the pGL3-Promoter luciferase reporter vector. The sequence of the region of wild-type (WT) *nqo1* containing the ARE is given (WT *nqo1* ARE). Above each nucleotide of the WT sequence is the individual mutation introduced in each case (i.e. the line designated 'Mutation'). Every base was mutated individually within the context of an otherwise WT sequence. RL-34 cells were transfected with each of the constructs (1 μg), and 16 h later they were treated with either 5 μM SUL or vehicle [0.1 % (v/v) DMSO; 'CTRL'] for a further 24 h. Cells were lysed and luciferase reporter assays were conducted. Values for vehicle-treated cells transfected with the WT ARE-containing reporter construct were arbitrarily set to 1.0, and other results were expressed relative to this. All results were normalized to *Renilla* luciferase internal control luminescence. Results are means ± S.D. for three separate experiments. Wild, the wild-type ARE-containing construct; 'pGL3P' represents luciferase reporter vector without insert. Asterisks represent mutations where no significant difference is observed between control and SUL treatments (at the 99 % confidence level).

Nrf2 is essential for NQO1 expression and binds, in recombinantly expressed form, the *nqo1* ARE as a heterodimer with small Maf protein

Previous data have demonstrated that the Nrf2 transcription factor is essential for both constitutive and oxidative-stress-inducible expression of murine NQO1 [7–9]. Consistent with these data, MEF cells derived from wild-type and *nrf2*$^{-/-}$ mice differ in their ability to support expression of NQO1. The oxidoreductase was both present constitutively and was increased substantially by SUL in wild-type cells. By contrast, it was undetectable under either condition in *nrf2*$^{-/-}$ MEFs (Figure 5A). At the mRNA level, wild-type MEFs showed a > 8-fold increase in NQO1 expression, following SUL treatment (Figure 5B). However, in *nrf2*$^{-/-}$ MEFs the level of NQO1 mRNA was reduced to 14 % of that seen in untreated wild-type cells, and there was a complete loss of induction upon treatment of cells with SUL (Figure 5B).

It is the ability of compounds such as SUL to affect nuclear accumulation of Nrf2 that is thought to account for their capacity to increase ARE-driven gene expression. Nrf2 has been shown to bind AREs in genes encoding certain detoxication enzymes, and is thereby thought to direct their expression [7]. The discovery that mouse *nqo1* contains an ARE provided a plausible link to explain the Nrf2-dependency of increased gene expression following exposure of cells to SUL. Indeed, artificial elevation of nuclear Nrf2 levels by heterologous expression provided additional support for this hypothesis. RL-34 and Hepa-1c1c7 cells were co-transfected with the wild-type and single-point mutant ARE reporter constructs described above, along with an expression vector for Nrf2 (Figures 6A and 6B). In keeping with data already presented, nucleotides highlighted for their integral role in induction of ARE-driven transcription by SUL, 5′-gagTcACaGTgAGtCggCAaaatt-3′ (Figure 4), were also found to be required for full response of the element to Nrf2 (Figures 6A and 6B).

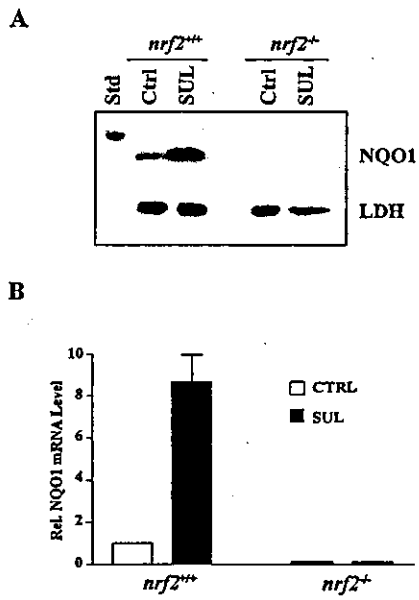

Figure 5 Constitutive and inducible NQO1 protein and mRNA expression is lost in *nrf2*$^{-/-}$ MEFs

(**A**) Western blot analysis of NQO1 in wild-type and *nrf2*$^{-/-}$ MEFs. Cell lines (as indicated) were treated for 24 h with either 5 μM SUL or vehicle [0.1 % (v/v) DMSO; 'Ctrl']. Following lysis, 10 μg of total cellular protein was resolved by SDS/PAGE and blotted with NQO1 or LDH antibodies. A His_6-tagged rat NQO1 standard (Std) is shown. (**B**) TaqMan® analysis of NQO1 mRNA levels. Cell lines (as indicated) were treated for 24 h with 5 μM SUL or vehicle [0.1 % (v/v) DMSO; 'CTRL']. Following isolation of total RNA and reverse transcription, real-time PCR was conducted. Values from vehicle-treated wild-type MEFs were arbitrarily set to 1.0, and all other results were expressed relative to this. Values are means ± S.D. for three separate experiments.

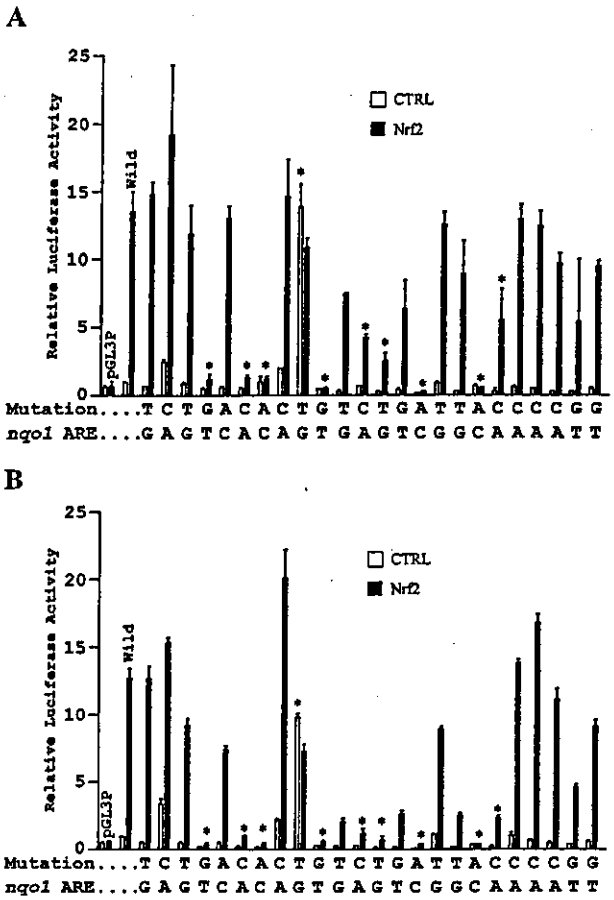

Figure 6 Nucleotide requirements for Nrf2 activation of the *nqo1* ARE by Nrf2 overexpression

(**A** and **B**) RL-34 and Hepa-1c1c7 cells respectively were transfected with single-point mutant ARE-reporter constructs (as described in the legend to Figure 4), along with either empty expression vector (CTRL) or expression vector containing Nrf2 cDNA (Nrf2). After transfection (48 h), cells were lysed and luciferase activities were measured. Wild, the wild-type ARE-containing construct; 'pGL3P' represents luciferase reporter vector without insert. Asterisks represent mutations that were previously shown (Figure 4) to cause complete loss of induction of luciferase activity by treatment of cells with SUL. Values for cells transfected with the wild-type ARE-containing reporter construct and empty expression vector were arbitrarily set to 1.0, and all other results were expressed relative to this. All results were normalized to *Renilla* luciferase internal control luminescence. Results are means ± S.D. for three separate experiments.

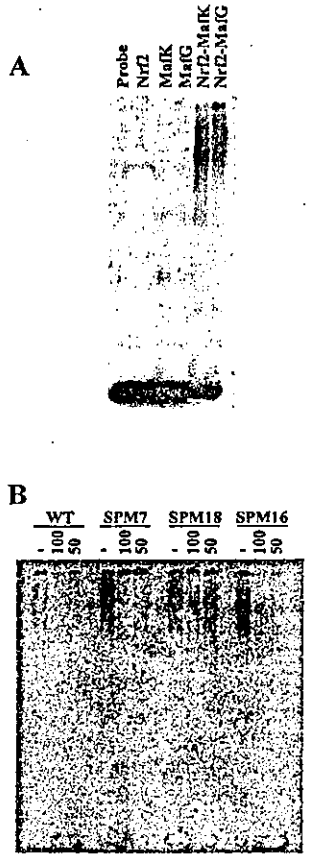

Figure 7 EMSA analyses of transcription factor binding to the *nqo1* ARE

(**A**) Binding of bacterially expressed Nrf2 and small Maf proteins to the ARE. Each of the proteins indicated was incubated individually, or in the combinations stated, with a 47 bp radiolabelled probe containing the *nqo1* ARE (corresponding to nt − 454 to − 414). Probe, reaction containing no protein. The autoradiograph shown is representative of results observed on at least three separate occasions. (**B**) Specificity of interaction between Nrf2–MafG and the *nqo1* ARE. Nrf2 and MafG proteins were incubated in combination in the absence (—) or presence of a 50- (50) or 100-fold (100) molar excess of unlabelled competitor DNA. WT, competitor was unlabelled wild-type ARE. SPM7 and SPM18, competitors were unlabelled single-point mutant AREs. These mutations were shown (Figure 4) to abolish ARE function, and were as follows: SPM7: 5′-GAGTCAAAGTGAGTCGGCAAAATT-3′ and SPM18: 5′-GAGTCACAGTGAGTCGGAAAAATT-3′. SPM16, competitor was an unlabelled single-point mutant ARE that was shown (Figure 4) to function similarly to the wild-type sequence: 5′-GAGTCACAGTGAGTCTGCAAAATT-3′. The autoradiograph shown is representative of results obtained on at least three separate occasions.

In order to establish that Nrf2 can interact directly with the mouse *nqo1* ARE, EMSAs were performed. Transcription factors of the bZIP family are required to form either homo- or heterodimers to allow DNA binding. Nrf2 cannot form homodimers, and its interaction with the ARE is thought to be achieved through heterodimerization with members of the small Maf family of transcriptional regulators, namely MafK and MafG [37]. These transcription factors were expressed in bacteria and assessed for their abilities to bind a radiolabelled *nqo1* ARE probe. When incubated separately, Nrf2, MafG and MafK were all incapable of interacting with the ARE (Figure 7A). By contrast, mixtures containing equal amounts of either Nrf2–MafG or Nrf2–MafK showed substantial *nqo1* ARE-binding activity (Figure 7A). Further support for regulation of the *nqo1* ARE by an Nrf2–Maf heterodimer was provided by EMSA competition experiments. A 50- or 100-fold molar excess of unlabelled wild-type *nqo1* ARE competed completely the Nrf2–MafG-shifted complex (Figure 7B). By contrast, two non-functional mutant forms of the *nqo1* ARE were not bound effectively by Nrf2–MafG (Figure 7B). Furthermore, an ARE containing a point mutation that did not affect the function of the element competed as well as the wild-type sequence for Nrf2–MafG interaction (Figure 7B). Identical results were obtained using Nrf2–MafK (results not shown).

SUL treatment of cell lines results in recruitment of an Nrf2–MafK heterodimer to the *nqo1* ARE

The above data indicate that oxidative stress ultimately results in binding of the *nqo1* ARE by a *trans*-acting transcriptional complex containing Nrf2 and small Maf. In order to test this hypothesis further, nuclear extracts were prepared from SUL- and vehicle-treated cell lines and analysed for their *nqo1* ARE-binding activity by EMSA. Two specific ARE-binding complexes, ARE-bc1 and ARE-bc3, were observed in extracts from vehicle-treated cells (Figure 8). These complexes were again present in nuclear protein from cells that had been exposed to SUL

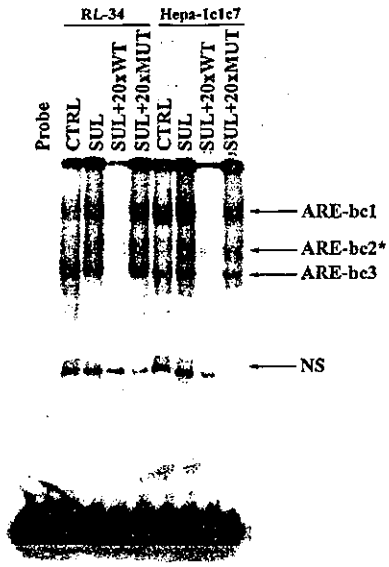

Figure 8 ARE-binding activity of RL-34 and Hepa-1c1c7 cell nuclear extracts

Nuclear extracts were prepared from the indicated cell lines following treatment with 5 μM SUL or vehicle [0.1 % (v/v) DMSO; 'CTRL'] for 4 h. Nuclear extract (7.5 μg of protein) was incubated with the 47 bp radiolabelled *nqo1* ARE probe defined in Figure 7. Three specific ARE-binding complexes were detected: ARE-bc1, ARE-bc2 and ARE-bc3: the asterisk represents complex induced by SUL treatment of cell lines; NS, non-specific complex; Probe, reaction containing no nuclear protein. Reactions were also conducted, using nuclear protein from SUL-treated cells, in the presence of a 20-fold molar excess of unlabelled wild-type ARE (SUL + 20 × WT) or a 20-fold molar excess of unlabelled mutant ARE (SUL + 20 × MUT). The mutant construct used contained a single-point mutation that abolished ARE-function in luciferase reporter assays (Figure 4): 5′-GAGTCACAGGGAGTCGGCAAAATT-3′. The autoradiograph shown is representative of results obtained on at least three separate occasions.

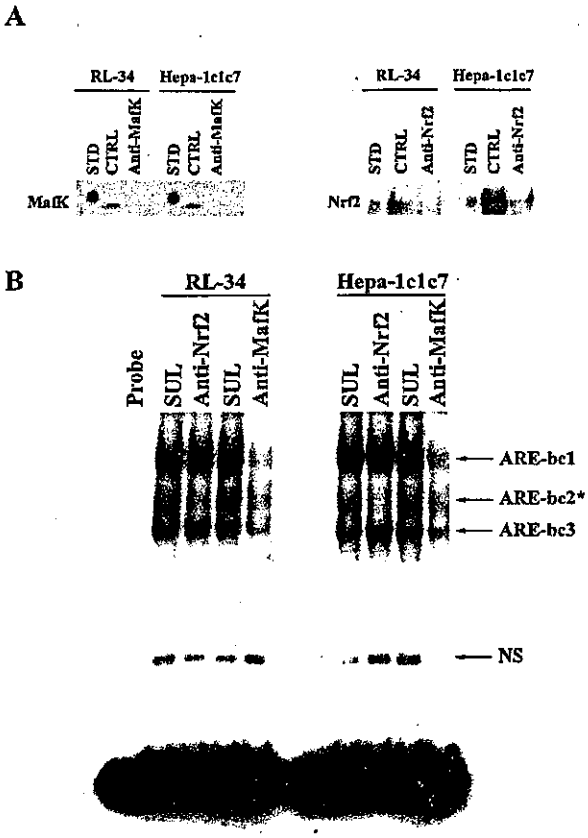

Figure 9 Analysis of ARE binding complexes by immunodepletion

(**A**) Western blot analysis of immunodepleted nuclear protein from RL-34 and Hepa-1c1c7 cells. Nuclear extracts were prepared from cells treated for 4 h with 5 μM SUL and depleted using either anti-Nrf2, anti-MafK or control rabbit IgG (CTRL), as indicated. Depleted nuclear extract (20 μg) was resolved by SDS/PAGE, and blotted using the antibodies indicated on the left of the figure. A His_6-tagged bacterially expressed standard (STD) was included in each case. (**B**) EMSA analysis of *nqo1* ARE-binding activity of depleted extracts. Control rabbit IgG (SUL), Nrf2- (anti-Nrf2) or MafK- (anti-MafK) depleted extracts, from the indicated cell-lines, were incubated with a 47 bp radiolabelled DNA fragment containing the *nqo1* ARE. The three specific ARE-binding complexes detected in Figure 8 are shown: ARE-bc1, ARE-bc2 and ARE-bc3. The asterisk represents complex induced by SUL treatment of cell lines; NS, non-specific complex; Probe, reaction containing no nuclear protein. The autoradiograph shown is representative of results obtained on at least three separate occasions.

(Figure 8); however, an additional ARE-binding complex, ARE-bc2, was also observed (Figure 8). This result indicated that ARE-bc2 represented the *trans*-acting factor(s) responsible for transcriptional activation of *nqo1* through the ARE.

The specificity of binding of the above complexes was ensured by EMSA competition experiments. A 20-fold molar excess of unlabelled wild-type ARE competed the shifted bands, whereas a mutated ARE sequence was unable to do the same (Figure 8).

Immunodepletion experiments were performed to determine the identity of transcription factors within ARE-bc2. Nrf2 and MafK were individually depleted from nuclear extracts prepared from SUL-treated cells (Figure 9A). The resulting extracts were analysed by EMSA. Depletion of Nrf2 resulted in a loss of ARE-bc2, but had no effect on levels of either ARE-bc1 or ARE-bc3, when compared with extract depleted with control antibody (Figure 9B). The level of ARE-bc2 was also substantially diminished by immunodepletion of MafK in nuclear extracts (Figure 9B). These results support the hypothesis that the transcriptional complex recruited to and activating the *nqo1* ARE consists, at least in part, of an Nrf2–MafK heterodimer. Interestingly, MafK-depleted extracts also demonstrated a loss of the two additional specific ARE-binding complexes, ARE-bc1 and ARE-bc3 (Figure 9B). Thus MafK may also regulate the *nqo1* ARE through dimerization with factors other than Nrf2.

Nrf2 and MafK interact with the *nqo1* ARE *in vivo*

In order to evaluate the biological significance of the EMSA binding data, ChIP experiments were performed. Immunoprecipitations were carried out on formaldehyde-fixed protein–DNA complexes isolated from SUL- and vehicle-treated Hepa-1c1c7 cells. The association of the protein of interest with the *nqo1* ARE was then assessed by PCR using primers specific for this region of the gene. Nrf2 antibody was used to precipitate the bZIP protein cross-linked to DNA from both vehicle- and SUL-treated cells. Portions of DNA containing the *nqo1* ARE were precipitated from vehicle-treated Hepa-1c1c7 cells; however, following SUL treatment, the signal obtained was far greater, indicating substantial recruitment of Nrf2 to the ARE (Figure 10). Binding of MafK to the *nqo1* ARE, under the conditions described for Nrf2, was also assessed. MafK was found to be strongly associated with the ARE in both SUL- and vehicle-treated Hepa-1c1c7 cells (Figure 10). Although there was some indication of MafK recruitment, this was not as pronounced as the results observed for Nrf2. This finding probably reflects an ability of MafK to bind the *nqo1* ARE, not only with Nrf2, but also as part of constitutive ARE-binding complexes lacking this factor (as shown above by EMSA).

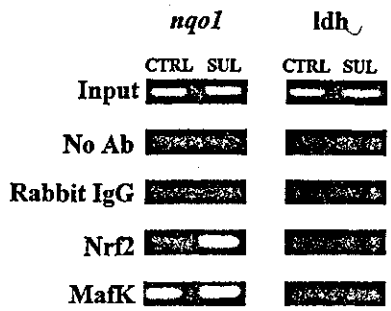

Figure 10 Analysis of Nrf2 and MafK binding to the *nqo1* ARE by ChIP assay

Hepa-1c1c7 cells were treated with 5 μM SUL or vehicle [0.1% (v/v) DMSO; 'CTRL'] for 4 h, before proteins were cross-linked to DNA through addition of formaldehyde directly to the culture medium. Cells were lysed, sonicated and immunoprecipitations were performed using no antibody (No Ab), control rabbit IgG (Rabbit IgG), anti-Nrf2 (Nrf2) or anti-MafK (MafK). A portion of material not subjected to immunoprecipitation was saved to act as a control for the amount of DNA added to each immunoprecipitate (Input). PCR reactions were conducted using primers specific for the region of the *nqo1* 5′-upstream region encompassing the ARE, or using oligonucleotides specific for the *ldh* promoter, as indicated. Results are representative of three separate experiments.

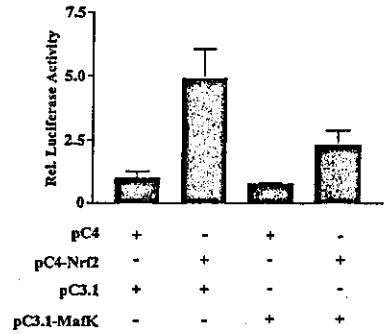

Figure 11 Overexpression of MafK represses ARE-driven *nqo1* transcription

RL-34 cells were transfected with expression vectors for Nrf2 and MafK or the respective empty constructs pC4 and pC3.1, as indicated. All cells were transfected with the −1016/*nqo5′–luc nqo1* ARE reporter construct generated in this study. After transfection (48 h), cells were lysed and luciferase reporter assays were conducted. Results are means ± S.D. for three separate experiments.

In all of these experiments, immunoprecipitations performed in the absence of IgG or using a control rabbit IgG failed to 'pull down' the *nqo1* ARE, thereby demonstrating the region of DNA of interest could not be enriched non-specifically (Figure 10). Also, PCR reactions using primers specific for the *ldh* (lactate dehydrogenase) promoter were all unsuccessful (Figure 10), ensuring no genomic DNA contamination of samples, while confirming the antibodies used were incapable of precipitating this non-specific region of the genome.

MafK overexpression affects transcriptional repression

To gain further insight into the role of the ARE-binding transcriptional complexes containing MafK, overexpression studies were performed. RL-34 cells were transiently transfected with expression plasmids for both Nrf2 and MafK, either alone or in combination, along with the *nqo1* 5′-upstream-region reporter construct, −1016/*nqo5′–luc*. In the absence of Nrf2-expressing plasmid, MafK had little effect on luciferase activity, with only a slight decrease observed (Figure 11). However, co-expression of MafK and Nrf2 resulted in repression of the transactivation observed when Nrf2 plasmid was transfected alone (Figure 11). These results indicate that MafK can form a heterodimeric complex capable of repressing ARE-driven gene transcription.

DISCUSSION

Biochemical and genetic data have demonstrated that NQO1 plays a fundamental role in combating oxidative stress invoked by xenobiotics [2–5]. This oxidoreductase forms part of a battery of cytoprotective genes, the expression of which is up-regulated upon cellular challenge with electrophilic chemicals. In this regard, induction of murine NQO1 in Hepa-1c1c7 cells is used in high-throughput screening of compounds to identify those with ability to stimulate cytoprotective gene expression [38,39]. However, the molecular mechanism by which transcription of this oxidoreductase is activated has not been reported previously.

The *nqo1* ARE

Our study of the sequence requirements of the *nqo1* ARE represents the first comprehensive single-nucleotide analysis of any such element. The ARE spans 24 bp (nt −444 to −421) and controls both constitutive and inducible *nqo1* expression. Our mutagenesis data define the element as comprising 5′-gagTcACa**GTgAGtCggC**Aaaatt-3′, where nucleotides shown in capital letters are those whose mutation results in a complete loss in response to SUL and those in bold represent the 'core' ARE, as most widely reported. It is likely that the bases in capitals represent those forming critical contacts with the Nrf2–Maf transcriptional complex.

Our analysis demonstrates the importance of nucleotides previously thought to be redundant in ARE function. Within the current consensus, five bases are denoted 'n': 5′-TMAnnRTGAYnnnGCRwwww-3′. Mutations introduced at two of these positions, 5′-gagTcA*C*a**GTgAGt***C***gg**CAaaatt-3′, shown underlined and italicized (with the core in bold), completely abolished induction. In addition, the thymine in the centre of the 'core' ARE (underlined and italicized in the following sequence), 5′-gagTcACa**GTgAG***t***CggC**Aaaatt-3′, at a position previously regarded as redundant, also makes a substantial contribution to the function of the ARE. Even though we have identified three nucleotides that make a hitherto unrecognized contribution to ARE function, we have also found that two guanines (5′-gagTcACa**GT***g***AGtCg-***g***C**Aaaatt-3′; guanines shown italicized and underlined) within the 'core' ARE make a less significant contribution to enhancer activity than was previously thought. Interestingly, the most 5′ of these two guanines has also been found to be variant in the human *GCLC* promoter [40].

Our observation that the cytosines in the *nqo1* ARE situated at positions equivalent to 'n' nucleotides in the consensus sequence are required for enhancer function does not discount the possibility that, within other elements, degeneracy may exist in the aforementioned bases. Importantly, we report here that introduction of certain bases present in other wild-type AREs into the corresponding position(s) of the *nqo1* enhancer abolishes function [12–18,20]. On the other hand, specific nucleotides that are not essential for activity of the *nqo1* ARE are central to the function of other elements (Table 1). Therefore different AREs have distinct sequence requirements.

Three explanations may rationalize the above findings. First, the sequence of a response element could manipulate the orientation of the activating transcriptional complex, as is the case for AP-1 (activator protein-1) sites [43], thereby influencing interaction

Table 1 Comparison of mouse, rat and human ARE enhancers

The upper-case letters represent nucleotides not critical for ARE function, as assessed by individual point mutations. Underlined upper-case letters show nucleotides found, by single-point mutation, to be essential for function of the ARE in question. Lower-case letters show nucleotides not mutated individually. The asterisks show mutations in the *nqo1* ARE that led to the introduction of nucleotides present in other ARE sequences and/or those permitted by the ARE consensus sequence. Alterations made are indicated in each case. Abbreviations used follow standard IUPAC nomenclature (M = A or C; R = A or G; Y = C or T; W = A or T; n = any nucleotide). EpRE, electrophile response element.

Gene/species	Enhancer	Sequence	Reference
		C* A* T* A*	
nqo1, mouse	ARE	GAGTCACA GTGAGTCGGCA AAATT	This study
NQO1, rat	ARE	gaGtCaCa GTGACttGGCA AAATC	[36]
gsta1, mouse	EpRE/ARE	tgcTAATG Gtgacaaagca ACTTT	[12,21]
GSTA2, rat	ARE	tGCTaAtG GTGACAAAGCA aactt	[20]
GCLM, human	EpRE/ARE	ggaagaca aTgactaAgca gaaat	[41]
GCLC, human	ARE4	gcctcccc gTgactcagcg ctttg	[18,42]
Previously proposed consensus		TMAnn RTGAYnnnGCR WWWW	[21]

with required cofactors. Secondly, the presence of a nucleotide in any given position may determine sequence requirements elsewhere in the ARE in order to bind Nrf2–Maf stably. Thirdly, certain ARE sequences may represent suboptimal binding sites to prevent transcription from being dominated by Nrf2–Maf. Further analysis is required to assess these possibilities.

Nrf2-controlled regulation of *nqo1* transcription

In the present study, the use of MEF cells allowed the unequivocal demonstration that Nrf2 is essential for both constitutive and SUL-inducible *nqo1* expression. Strikingly, in *nrf2*$^{-/-}$ cells, NQO1 protein was undetectable, and mRNA levels were barely obvious under any of the conditions tested. Both EMSA and ChIP experiments demonstrated convincingly that Nrf2 is recruited to the *nqo1* ARE following exposure of cells to SUL. We would further extrapolate this observation to conclude that exposure of cells to compounds capable of generating an oxidative stress is the stimulus that increases occupancy of the *nqo1* ARE by Nrf2. These data therefore provide an explanation for the perturbed expression of NQO1 observed in the *nrf2*$^{-/-}$ mouse.

Fibroblasts prepared from *nrf1*$^{-/-}$ mouse embryos express significantly less GCLC and GCLM than their wild-type counterparts [44]. Exposure of *nrf1*$^{-/-}$ MEFs to paraquat results in the accumulation of free radicals to a much greater extent than in *nrf1*$^{+/+}$ MEFs treated in a similar fashion [44]. We have found that the expression of GCLC and GCLM is reduced in *nrf2*$^{-/-}$ MEFs (L. Higgins, L. I. McLellan, M. Yamamoto and J. D. Hayes, unpublished work), and would predict that the Nrf2-nulled cells will be more sensitive to oxidative stress. This hypothesis remains to be tested. However, we did check that the dose of SUL used to treat *nrf2*$^{-/-}$ MEFs (Figure 5) was not toxic.

The mechanism by which Nrf2 affects transcriptional activation of ARE-driven genes is not fully understood. It is likely that binding of Nrf2 to an ARE augments association of RNA polymerase II with the core promoter either through direct interaction with components of the basic transcription apparatus or via the co-activator protein CBP (CREB-binding protein) [45]. Indeed, the involvement of cofactors is consistent with our hypothesis that the ARE sequence may influence the architecture of bound Nrf2–Maf, and thereby manipulate their abilities to interact with other proteins and hence alter the capacity to activate transcription.

Small-Maf-mediated negative regulation of *nqo1* transcription

We have shown that MafK facilitates transcriptional activation of *nqo1* by heterodimerizing with Nrf2, and thereby allowing ARE binding. However, overexpression of MafK repressed Nrf2-mediated transcription. This observation is consistent with the findings of other groups that have shown inhibition of ARE-driven transcription by heterologous expression of small Maf [27–29]. Our EMSA and ChIP analyses have shown that MafK binds the *nqo1* ARE as part of protein complexes either containing or lacking Nrf2. Under constitutive conditions, only MafK-containing complexes lacking Nrf2 were observed. On the basis of these data, we propose that constitutively present EMSA complexes, ARE-bc1 and ARE-bc3, which lack Nrf2 but contain MafK are transcriptional repressors. In the RL-34 cell line, constitutive *nqo1* transcription is very low and MafK expression had little effect, indicating that the gene is already held in a repressed state. Increased levels of Nrf2 within the nucleus would compete with a MafK-containing repressor complex for binding to the ARE. Overexpression of MafK could antagonize this in a number of ways. However, we hypothesize that the majority of Nrf2 molecules present in the nucleus exist as heterodimers with small Maf protein. This would mean that introduction of further MafK could only serve to confer DNA binding capacity upon the repressive complexes. The identity of the partner molecules of MafK within ARE-bc1 and ARE-bc3 remains to be elucidated, although Bach-1 [46] and Bach-2 represent likely candidates.

Concluding comments

The results reported herein provide a molecular mechanism for transcriptional activation of *nqo1* by electrophilic xenobiotics. They also give an in-depth analysis into the ARE, both in terms of the sequence requirements of such elements and the protein complexes involved in their regulation. Our critical reassessment of the ARE consensus sequence has shown that nucleotides thought to be redundant in ARE function have integral roles in the activity of the *nqo1* *cis*-element. A model is described for transcriptional activation of *nqo1* via its ARE. Under constitutive conditions, the ARE is bound by a repressive heterodimer consisting of MafK and an as-yet-unidentified protein. Exposure of cells to oxidative stress results in accumulation of Nrf2 within the nucleus and recruitment of this factor to the ARE, as a heterodimer with MafK, replacing the repressor complex.

We are indebted to Dr Brian McStay (Biomedical Research Centre, University of Dundee) for expert advice throughout this study. We also thank Dr Simon A. Chanas (also of the Biomedical Research Centre) for providing bacterial expression vectors for Nrf2 and small Maf proteins. This work was supported by a Medical Research Council PhD studentship (G78/6808) awarded to P.N. and an MRC Component Grant (G0000268) to J.D.H. and Dr Clifford R. Elcombe (of the Biomedical Research Centre). M. McM was supported by a grant from the Association for International Cancer Research (99–041) awarded to M.Y. and J.D.H.

REFERENCES

1 Hayes, J. D., Ellis, E. M., Neal, G. E., Harrison, D. J. and Manson, M. M. (1999) Cellular response to cancer chemopreventive agents: contribution of the antioxidant responsive element to the adaptive response to oxidative and chemical stress. Biochem. Soc. Symp. **64**, 141–168

2 Dinkova-Kostova, A. T. and Talalay, P. (2000) Persuasive evidence that quinone reductase type 1 (DT diaphorase) protects cells against the toxicity of electrophiles and reactive forms of oxygen. Free Radical Biol. Med. **29**, 231–240

3 Ross, D., Kepa, J. K., Winski, S. L., Beall, H. D., Anwar, A. and Siegel, D. (2000) NAD(P)H:quinone oxidoreductase 1 (NQO1): chemoprotection, bioactivation, gene regulation and genetic polymorphisms. Chem.-Biol. Interact. **129**, 77–97

4 Long, II, D. J., Waikel, R. L., Wang, X.-J., Perlaky, L., Roop, D. R. and Jaiswal, A. K. (2000) NAD(P)H:quinone oxidoreductase 1 deficiency increases susceptibility to benzo(*a*)pyrene-induced mouse skin carcinogenesis. Cancer Res. **60**, 5913–5915

5 Radjendirane, V., Joseph, P., Lee, Y.-H., Kimura, S., Klein-Szanto, A. J. P., Gonzalez, F. J. and Jaiswal, A. K. (1998) Disruption of the DT diaphorase (NQO1) gene in mice leads to increased menadione toxicity. J. Biol. Chem. **273**, 7382–7389

6 Chanas, S. A., Jiang, Q., McMahon, M., McWalter, G. K., McLellan, L. I., Elcombe, C. R., Henderson, C. J., Wolf, C. R., Moffat, G. J., Itoh, K., Yamamoto, M. and Hayes, J. D. (2002) Loss of the Nrf2 transcription factor causes a marked reduction in constitutive and inducible expression of the glutathione S-transferase Gsta1, Gsta2, Gstm1, Gstm2, Gstm3 and Gstm4 genes in the livers of male and female mice. Biochem. J. **365**, 405–416

7 Itoh, K., Chiba, T., Takahashi, S., Ishii, T., Igarashi, K., Katoh, Y., Oyake, T., Hayashi, N., Satoh, K., Hatayama, I., Yamamoto, M. and Nabeshima, Y.-i. (1997) An Nrf2/small Maf heterodimer mediates the induction of phase II detoxifying enzyme genes through antioxidant response elements. Biochem. Biophys. Res. Commun. **236**, 313–322

8 McMahon, M., Itoh, K., Yamamoto, M., Chanas, S. A., Henderson, C. J., McLellan, L. I., Wolf, C. R., Cavin, C. and Hayes, J. D. (2001) The Cap'n'Collar basic leucine zipper transcription factor Nrf2 (NF-E2 p45-related factor 2) controls both constitutive and inducible expression of intestinal detoxification and glutathione biosynthetic enzymes. Cancer Res. **61**, 3299–3307

9 Thimmulappa, R. K., Mai, K. H., Srisuma, S., Kensler, T. W., Yamamoto, M. and Biswal, S. (2002) Identification of Nrf2-regulated genes induced by the chemopreventive agent sulforaphane by oligonucleotide microarray. Cancer Res. **62**, 5196–5203

10 Kwak, M.-K., Wakabayashi, N., Itoh, K., Motohashi, H., Yamamoto, M. and Kensler, T. W. (2003) Modulation of gene expression by cancer chemopreventive dithiolethiones through the Keap1-Nrf2 pathway. Identification of novel gene clusters for cell survival. J. Biol. Chem. **278**, 8135–8145

11 Lee, J.-M., Calkins, M. J., Chan, K., Kan, Y. W. and Johnson, J. A. (2003) Identification of the NF-E2-related factor-2-dependent genes conferring protection against oxidative stress in primary cortical astrocytes using oligonucleotide microarray analysis. J. Biol. Chem. **278**, 12029–12038

12 Friling, R. S., Bergelson, S. and Daniel, V. (1992) Two adjacent AP-1-like binding sites form the electrophile-responsive element of the murine glutathione S-transferase Ya subunit gene. Proc. Natl. Acad. Sci. U.S.A. **89**, 668–672

13 Inamdar, N. M., Ahn, Y. I. and Alam, J. (1996) The heme-responsive element of the mouse heme oxygenase-1 gene is an extended AP-1 binding site that resembles the recognition sequences for MAF and NF-E2 transcription factors. Biochem. Biophys. Res. Commun. **221**, 570–576

14 Tsuji, Y., Ayaki, H., Whitman, S. P., Morrow, C. S., Torti, S. V. and Torti, F. M. (2000) Coordinate transcriptional and translational regulation of Ferritin in response to oxidative stress. Mol. Cell. Biol. **20**, 5818–5827

15 Rushmore, T. H., King, R. G., Paulson, K. E. and Pickett, C. B. (1990) Regulation of glutathione *S*-transferase Ya subunit gene expression: identification of a unique xenobiotic-responsive element controlling inducible expression by planar aromatic compounds. Proc. Natl. Acad. Sci. U.S.A. **87**, 3826–3830

16 Favreau, L. V. and Pickett, C. B. (1991) Transcriptional regulation of the rat NAD(P)H:quinone reductase gene. Identification of regulatory elements controlling basal level expression and inducible expression by planar aromatic compounds and phenolic antioxidants. J. Biol. Chem. **266**, 4556–4561

17 Jaiswal, A. K. (1991) Human NAD(P)H:Quinone Oxidoreductase (NQO1) gene structure and induction by dioxin. Biochemistry **30**, 10647–10653

18 Mulcahy, R. T., Wartman, M. A., Bailey, H. H. and Gipp, J. J. (1997) Constitutive and β-naphthoflavone-induced expression of the human γ-glutamylcysteine synthetase heavy subunit gene is regulated by a distal antioxidant response element/TRE sequence. J. Biol. Chem. **272**, 7445–7454

19 Nguyen, T., Sherratt, P. J. and Pickett, C. B. (2003) Regulatory mechanisms controlling gene expression mediated by the antioxidant response element. Annu. Rev. Pharmacol. Toxicol. **43**, 233–260

20 Rushmore, T. H., Morton, M. R. and Pickett, C. B. (1991) The antioxidant responsive element. Activation by oxidative stress and identification of the DNA consensus sequence required for functional activity. J. Biol. Chem. **266**, 11632–11639

21 Wasserman, W. W. and Fahl, W. E. (1997) Functional antioxidant responsive elements. Proc. Natl. Acad. Sci. U.S.A. **94**, 5361–5366

22 Cho, H.-Y., Jedlicka, A. E., Reddy, S. P. M., Kensler, T. W., Yamamoto, M., Zhang, L.-Y. and Kleeberger, S. R. (2002) Role of Nrf2 in protection against hyperoxic lung injury in mice. Am. J. Respir. Cell Mol. Biol. **26**, 175–182

23 Stewart, D., Killeen, E., Naquin, R., Alam, S. and Alam, J. (2003) Degradation of transcription factor Nrf2 via the ubiquitin-proteasome pathway and stabilization by cadmium. J. Biol. Chem. **278**, 2396–2402

24 Nguyen, T., Sherratt, P. J., Huang, H.-C., Yang, C. S. and Pickett, C. B. (2003) Increased protein stability as a mechanism that enhances Nrf2-mediated transcriptional activation of the antioxidant response element. Degradation of Nrf2 by the 26 S proteasome. J. Biol. Chem. **278**, 4536–4541

25 Itoh, K., Wakabayashi, N., Katoh, Y., Ishii, T., O'Connor, T. and Yamamoto, M. (2003) Keap1 regulates both cytoplasmic-nuclear shuttling and degradation of Nrf2 in response to electrophiles. Genes Cells **8**, 379–391

26 McMahon, M., Itoh, K., Yamamoto, M. and Hayes, J. D. (2003) Keap1-dependent proteasomal degradation of transcription factor Nrf2 contributes to the negative regulation of antioxidant response element-driven gene expression. J. Biol. Chem. **278**, 21592–21600

27 Nguyen, T., Huang, H.-C. and Pickett, C. B. (2000) Transcriptional regulation of the antioxidant response element. Activation by Nrf2 and repression by MafK. J. Biol. Chem. **275**, 15466–15473

28 Dhakshinamoorthy, S. and Jaiswal, A. K. (2000) Small Maf (MafG and MafK) proteins negatively regulate antioxidant response element-mediated expression and antioxidant induction of the NAD(P)H:quinone oxidoreductase1 gene. J. Biol. Chem. **275**, 40134–40141

29 Wild, A. C., Moinova, H. R. and Mulcahy, R. T. (1999) Regulation of γ-glutamylcysteine synthetase subunit gene expression by the transcription factor Nrf2. J. Biol. Chem. **274**, 33627–33636

30 Tiemann, F. and Deppert, W. (1994) Immortalization of BALB/c mouse embryo fibroblasts alters SV40 large T-antigen interactions with the tumor suppressor p53 and results in a reduced SV40 transformation-efficiency. Oncogene **9**, 1907–1915

31 Plumb, J. A., Milroy, R. and Kaye, S. B. (1989) Effects of the pH dependence of 3-(4,5-dimethylthiazol-2-yl)-2,5-diphenyl-tetrazolium bromide-formazan absorption on chemosensitivity determined by a novel tetrazolium-based assay. Cancer Res. **49**, 4435–4440

32 Osoegawa, K., Tateno, M., Woon, P. Y., Frengen, E., Mammoser, A. G., Catanese, J. J., Hayashizaki, Y. and deJong, P. J. (2000) Bacterial artificial chromosome libraries for mouse sequencing and functional analysis. Genome Res. **10**, 116–128

33 Kelly, V. P., Ellis, E. M., Manson, M. M., Chanas, S. A., Moffat, G. J., McLeod, R., Judah, D. J., Neal, G. E. and Hayes, J. D. (2000) Chemoprevention of aflatoxin B_1 hepatocarcinogenesis by coumarin, a natural benzopyrone that is a potent inducer of aflatoxin B_1-aldehyde reductase, the glutathione S-transferase A5 and P1 subunits, and NAD(P)H:quinone oxidoreductase in rat liver. Cancer Res. **60**, 957–969

34 Boyd, K. E., Wells, J., Gutman, J., Bartley, S. M. and Farnham, P. J. (1998) c-Myc target gene specificity is determined by a post-DNA-binding mechanism. Proc. Natl. Acad. Sci. U.S.A. **95**, 13887–13892

35 Zhang, Y., Talalay, P., Cho, C. G. and Posner, G. H. (1992) A major inducer of anticarcinogenic protective enzymes from broccoli: isolation and elucidation of structure. Proc. Natl. Acad. Sci. U.S.A. **89**, 2399–2403

36 Favreau, L. V. and Pickett, C. B. (1995) The rat quinone reductase antioxidant response element. Identification of the nucleotide sequence required for basal and inducible activity and detection of antioxidant response element-binding proteins in hepatoma and non-hepatoma cell lines. J. Biol. Chem. **270**, 24468–24474

37 Motohashi, H., O'Connor, T., Katsuoka, F., Engel, J. D. and Yamamoto, M. (2002) Integration and diversity of the regulatory network composed of Maf and CNC families of transcription factors. Gene **294**, 1–12

38 Prochaska, H. J., Santamaria, A. B. and Talalay, P. (1992) Rapid detection of inducers of enzymes that protect against carcinogens. Proc. Natl. Acad. Sci. U.S.A. **89**, 2394–2398

39 Dinkova-Kostova, A. T., Abeygunawardana, C. and Talalay, P. (1998) Chemoprotective properties of phenylpropenoids, bis(benzylidene)cycloalkanones, and related Michael reaction acceptors: correlation of potencies as phase 2 enzyme inducers and radical scavengers. J. Med. Chem. **41**, 5287–5296

40 Erickson, A. M., Nevarea, Z., Gipp, J. J. and Mulcahy, R. T. (2002) Identification of a variant antioxidant response element in the promoter of the human glutamate-cysteine ligase modifier subunit gene. Revision of the ARE consensus sequence. J. Biol. Chem. **277**, 30730–30737

41 Moinova, H. R. and Mulcahy, R. T. (1998) An electrophile responsive element (EpRE) regulates β-naphthoflavone induction of the human γ-glutamylcysteine synthetase regulatory subunit gene. Constitutive expression is mediated by an adjacent AP-1 site. J. Biol. Chem. **273**, 14683–14689

42 Wild, A. C., Gipp, J. J. and Mulcahy, R. T. (1998) Overlapping antioxidant response element and PMA response element sequences mediate basal and β-naphthoflavone-induced expression of the human γ-glutamylcysteine synthetase catalytic subunit gene. Biochem. J. **332**, 373–381

43 Ramirez-Carrozzi, V. and Kerppola, T. (2003) Asymmetric recognition of non-consensus AP-1 sites by Fos-Jun and Jun-Jun influences transcriptional cooperativity with NFAT1. Mol. Cell. Biol. **23**, 1737–1749
44 Kwong, M., Kan, Y. W. and Chan, J. Y. (1999) The CNC basic leucine zipper factor, Nrf1, is essential for cell survival in response to oxidative stress-inducing agents. Role for Nrf1 in γ-*gcs*$_L$ and *gss* expression in mouse fibroblasts. J. Biol. Chem. **274**, 37491–37498
45 Katoh, Y., Itoh, K., Yoshida, E., Miyagishi, M., Fukamizu, A. and Yamamoto, M. (2001) Two domains of Nrf2 cooperatively bind CBP, a CREB binding protein, and synergistically activate transcription. Genes Cells **6**, 857–868
46 Sun, J., Hoshino, H., Takaku, K., Nakajima, O., Muto, A., Suzuki, H., Tashiro, S., Takahashi, S., Shibahara, S., Alam, J. et al. (2002) Hemoprotein Bach1 regulates enhancer availability of heme oxygenase-1 gene. EMBO J. **21**, 5216–5224

Received 22 May 2003/17 June 2003; accepted 20 June 2003
Published as BJ Immediate Publication 20 June 2003, DOI 10.1042/BJ20030754

Free Radical Biology & Medicine, Vol. 35, No. 1, pp. 102–113, 2003

0891-5849/03/$–see front matter

ELSEVIER

doi:10.1016/S0891-5849(03)00269-7

Original Contribution

A POTENTIAL MECHANISM FOR THE IMPAIRMENT OF NITRIC OXIDE FORMATION CAUSED BY PROLONGED ORAL EXPOSURE TO ARSENATE IN RABBITS

JINGBO PI,*†[1] SATOMI HORIGUCHI,‡ YANG SUN,* MASATOSHI NIKAIDO,‡ NOBUHIRO SHIMOJO,§ TOSHIO HAYASHI,‖ HIROSHI YAMAUCHI,¶ KEN ITOH,# MASAYUKI YAMAMOTO,# GUIFAN SUN,† MICHAEL P. WAALKES,** and YOSHITO KUMAGAI§

*Graduate School Doctoral Program in Medical Sciences, University of Tsukuba, Tsukuba, Ibaraki, Japan; †Department of Labor Hygiene and Occupational Health, School of Public Health, China Medical University, Shenyang, China; ‡Master's Program in Environmental Sciences and §Department of Environmental Medicine, Institute of Community Medicine, University of Tsukuba, Tsukuba, Ibaraki, Japan; ‖Department of Geriatrics, Nagoya University School of Medicine, Nagoya, Japan; ¶Department of Preventive Medicine, St. Marianna University School of Medicine, Kawasaki, Japan; #Center for Tsukuba Advanced Research Alliance, University of Tsukuba, Tsukuba, Ibaraki, Japan; and **Inorganic Carcinogenesis Section, Laboratory of Comparative Carcinogenesis, NCI at NIEHS, NIH, Research Triangle Park, NC, USA

(*Received* 21 *January* 2003; *Revised* 31 *March* 2003; *Accepted* 17 *April* 2003)

Abstract—We have recently found evidence for impairment of nitric oxide (NO) formation and induction of oxidative stress in residents of an endemic area of chronic arsenic poisoning in Inner Mongolia, China. To investigate the underlying mechanisms responsible for these phenomena, a subchronic animal experiment was conducted using male New Zealand White rabbits. After 18 weeks of continuous exposure of rabbits to 5 mg/l of arsenate in drinking water, a significant decrease in systemic NO production occurred, as shown by significantly reduced plasma NO metabolites levels (76% of control) and a tendency towards decreased serum cGMP levels (81.4% of control). On the other hand, increased oxidative stress, as shown by significantly increased urinary hydrogen peroxide (H_2O_2) (120% of control), was observed in arsenate-exposed rabbits. In additional experiments measuring aortic tension, the addition of either the calcium ionophore A23187 or acethylcholine (ACh) induced a transient vasoconstriction of aortic rings prepared from arsenate-exposed rabbits, but not in those prepared from control animals. This calcium-dependent contractility action observed in aorta rings from arsenate-exposed rabbits was markedly attenuated by the superoxide ($O_2^{\bullet -}$) scavenging enzyme Cu, Zn-SOD, as well as diphenyleneiodonium (DPI) or N^G-nitro-L-arginine methyl ester (L-NAME), which are inhibitors for nitric oxide synthase (NOS). However, the cyclooxygenase inhibitor indomethacin or the xanthine oxidase blocker allopurinol had no effect on this vasoconstriction. These results suggest that arsenate-mediated reduction of systemic NO may be associated with the enzymatic uncoupling reaction of NOS with a subsequent enhancement of reactive oxygen species such as $O_2^{\bullet -}$, an endothelium-derived vasoconstricting factor. Furthermore, hepatic levels of (6*R*)-5,6,7,8-tetrahydro-L-biopterin (BH_4), a cofactor for NOS, were markedly reduced in arsenate-exposed rabbits to 62% of control, while no significant change occurred in cardiac L-arginine levels. These results suggest that prolonged exposure of rabbits to oral arsenate may impair the bioavailability of BH_4 in endothelial cells and, as a consequence, disrupt the balance between NO and $O_2^{\bullet -}$ produced from endothelial NOS, such that enhanced free radicals are produced at the expense of NO. © 2003 Elsevier Inc.

Keywords—Arsenate, Free radicals, Nitric oxide, Superoxide, Tetrahydrobiopterin, Vasoconstriction, Rabbit, Oral exposure

Address correspondence to: Yoshito Kumagai, Ph.D., Department of Environmental Medicine, Institute of Community Medicine, University of Tsukuba, 1-1-1 Tennodai, Tsukuba, Ibaraki 305-8575, Japan; Tel: +81 (298) 53-3133; Fax: +81 (298) 53-3133; E-Mail: yk-em-tu@md.tsukuba.ac.jp.

[1]Current address: Inorganic Carcinogenesis Section, Laboratory of Comparative Carcinogenesis, NCI at NIEHS, NIH, Mail Drop F0-09, 111 Alexander Drive, Research Triangle Park, NC 27709, USA.

INTRODUCTION

Arsenic is a naturally occurring element that is present in the environment in both organic and inorganic forms [1]. Human exposures to the generally more toxic inorganic arsenic compounds occur in occupational or environmental settings, as well as through medicinal arsenical use [2,3]. Exposure through consumption of drinking water containing elevated concentrations of arsenic, primarily from natural contamination, is the main source of human environmental exposure in most populations worldwide [4–14]. Prolonged exposure to arsenic through consuming contaminated drinking water results in many chronic diseases, including vascular diseases such as peripheral- and cardio-vascular disease, arteriosclerosis, Raynaud's syndrome, and hypertension [15–20]. Oral exposure to inorganic arsenic in humans is also associated with the development of pronounced skin lesions [9] and increase the incidence of cancer at a variety of sites [2,20,21].

Nitric oxide (NO) produced in endothelial cells is involved in the regulation of blood pressure, inhibition of the adhesion of leukocytes to the endothelium, interactions between platelets and the vessel wall, and proliferation and migration of vascular smooth muscle cells [22,23]. Decreased availability of biologically active NO in the endothelium is implicated in the pathophysiology of several vascular diseases. Major risk factors for atherosclerotic vascular disease, such as hypercholesterolemia, atherosclerosis, and peripheral arterial occlusive disease, have all been associated with impaired NO bioactivity [24,25]. Our recent epidemiological investigation in Inner Mongolia indicated that serum levels of nitrite/nitrate, the stable metabolites of endogenous NO, were almost 50% lower in patients chronically exposed to elevated arsenic in the drinking water than in control subjects, suggesting arsenic-induced vascular disorders may be attributable, at least in part, to impairment of NO production [7]. Furthermore, oxidative stress, as indicated by the increase of serum lipid peroxides, was also observed in the chronic arsenic-exposed patients [26]. In this regard, it has been shown that inorganic arsenate (iAs[V]) or arsenite (iAs[III]) suppresses the activity of endothelial NO synthase (eNOS) in human umbilical vein endothelial cells, suggesting the direct inhibition of eNOS by inorganic arsenicals may be one cause of the significant decrease of NO production in vivo [7]. However, the precise mechanistic details of the basis of decreased NO production induced by chronic oral inorganic arsenic exposure remain unknown.

Constitutive nitric oxide synthase (cNOS), including the endothelial- and neuronal- isoform, constitutively produces both NO and, under certain conditions, superoxide ($O_2^{\bullet -}$) [27,28]. The key in the net outcome of NO production by cNOS appears to be the presence of the cofactor (6*R*)-5,6,7,8-tetrahydro-L-biopterin (BH_4) and the physiological precursor of NO, L-arginine. BH_4 is an important allosteric effector of all NOS isoforms through stabilization of the dimeric, active form of the enzymes, and may play a key role in the control of the calcium-dependent production of NO and $O_2^{\bullet -}$ in vivo [29]. An insufficiency of BH_4 leads to uncoupling of the L-arginine-NO pathway, resulting in decreased NO production accompanied by increased formation of $O_2^{\bullet -}$ and hydrogen peroxide (H_2O_2) [30,31]. cNOS also catalyses the uncoupled reduction of oxygen in the absence of L-arginine, leading to the production of $O_2^{\bullet -}$ and H_2O_2 [24]. L-arginine metabolites, $N^{G,\,NG}$-dimethyl-L-arginine (ADMA) and N^G–methyl-L-arginine (L-NMMA), are capable of competitively inhibiting cellular L-arginine uptake and cNOS activity [32,33], and a diminished availability of cellular L-arginine or the accumulation of endogenous inhibitors of cNOS leads to decreased NO production. A decreased L-arginine/ADMA ratio in blood is, in fact, associated with many vascular diseases [34,35].

Although there is no description of a direct relationship between arsenic exposure and disrupted function of BH_4, clinical evidence suggests that chronic arsenic exposure may disturb the crucial functions of this cofactor, leading to clinical manifestations. Beyond its involvement with cNOS, BH_4 is an essential electron donor for the hydroxylation of the aromatic amino acids, which are regarded as key processes in the biosynthesis of skin pigments as well as several neurotransmitters, including catecholamines and serotonin [36]. Cutaneous disorders of pigmentation are the most common manifestations of chronic arsenic poisoning [9,13] and arsenic-induced impairment of catechoamines production has been reported previously [37–39]. McDorman et al. [40] recently reported that dietary folate deficiency enhances induction of micronuclei by arsenic in mice, whereas folates have been suggested to stimulate endogenous BH_4 regeneration [41].

In the present study, we hypothesized that chronic arsenic exposure may affect availabilities of BH_4 and/or L-arginine, thereby reducing systemic NO production and increasing release of $O_2^{\bullet -}$ by creating an imbalance between NO and $O_2^{\bullet -}$ production. To test this hypothesis, rabbits, which have been reported to biotransform arsenic in a manner very similar to humans [42], were exposed to arsenate through the drinking water, and changes in systemic production of NO, as well as BH_4 and L-arginine and its methylated metabolites, were measured. Because $O_2^{\bullet -}$ is a potent inducer of endothelium-dependent vasoconstriction

and itself can inactivate NO [43], our second goal was to investigate the alteration in vascular tone and contractility of aortas with intact endothelium, using an aortic ring organ bath system.

MATERIALS AND METHODS

Animals and study design

Six week old male New Zealand White rabbits (Kitayama Rabesu Co., Nagano, Japan) weighing 1.4–1.6 kg were individually housed in an environmentally controlled room with a 12 h light/dark cycle and free access to a standard laboratory chow CR-3 (Nippon Clea Co. Ltd., Tokyo, Japan). The experimental treatment protocol used in this study was approved by the Animal Care and Use Committee of the University of Tsukuba. All procedures were in accordance with institutional guidelines for animal studies. Drinking water solutions were made with distilled water. The animals were randomly divided into two groups of 6 animals each and were allowed ad libitum drinking water containing 5 mg arsenic/l (as As[V]) or untreated drinking water (control group). Exposure was continuous for 18 weeks. Arsenate drinking water solution was made up fresh weekly using Na_2HAsO_4 (Kishida Chemical Co., Osaka, Japan) in distilled water. The general appearance of the rabbits was observed daily. Daily water and weekly chow consumption were measured. Body weights were monitored weekly. At the end of week 18, after 24 h samples of urine were taken by using metabolic cages with the sample bottles kept on ice during the collection, blood samples were taken from central ear arteries after 24 h of fasting, and plasma was separated immediately. The animals were then killed by injection of air into ear vein, the tissues were extracted immediately, frozen in liquid nitrogen, and stored at −70°C until use.

Measurement of nitrite and nitrate in plasma

Because NO has a very short half-life, it has been quantified indirectly in most studies by measuring the stable NO metabolites nitrite and nitrate. Combined nitrite and nitrate levels in plasma were determined by the method of Green et al. [44], with slight modification. Briefly, after nitrate was reduced to nitrite with 0.2 U/ml *Aspergillus* nitrate reductase (Sigma Chemical Co., St. Louis, MO, USA) in the presence of 0.1 μM FAD and 10 μM NADPH, the mixture was reacted with Griess reagent (1 ml) consisting of 1% sulfanilamide and 0.1% N-(1-naphtyl)-ethylenediamine HCl in 5% H_3PO_4. The resulting sample was measured at 540 nm with $NaNO_2$ as a standard.

Radioimmunoassay for cyclic guanosine monophosphate (cGMP) in plasma

Quantitative assay for cGMP in plasma was performed using a commercial radioimmunoassay kit (Amersham Pharmacia Biotech UK Ltd., Buckinghamshire, UK) after sample extraction. For extraction, plasma (50 μl) was diluted with deionized distilled water (DDW) (150 μl) and then mixed with an equal volume 10% of trichloroacetic acid (200 μl). After centrifuge at 15,000 × *g* for 10 min, 200 μl of the supernatant was extracted 4 times with 1.5 ml water-saturated diethyl ether by vigorous shaking for 1 min. The aqueous phase was dried at 60°C by N_2 gas and dissolved in 200 μl of 0.05 M sodium acetate buffer (pH 5.8), and then was acetylated with a mixture of acetic acid anhydride/triethylamine (1:2 by volume). A series of known levels of cGMP were extracted and acetylated as above to provide a standard for quantification.

Determination of H_2O_2 in urine

H_2O_2 in urine was determined using the method of ferrous oxidation-xylenol orange (FOX) assay [45]. Briefly, urine samples (150 μl) were mixed with 17 μl methanol, immediately followed by the addition of FOX reagent and mixing by vortex. The resulting solution was incubated at room temperature for 10 min and centrifuged at 15,000 × *g* for 5 min. Absorbance at 560 nm was monitored against a methanol blank. The concentration of H_2O_2 in standard stock solution was calculated using the extinction coefficient of 43.6 $mM^{-1}cm^{-1}$ at 240 nm. Creatinine levels in urine were determined by a commercially available Creatinine Test Kit (Wako Pure Chemical Industries, Osaka, Japan).

Isometric tension measurement in aortic rings

The thoracic aortic rings were prepared essentially as described by Furchgott and Zawadzki [46]. Briefly, the thoractic aortas were carefully removed to protect the endothelial lining, cleared of adhering fat and connective tissues, and cut into cylindrical segments approximately 2 mm in length. The rings were mounted under 1 g of resting tension on stainless-steel hooks in 10 ml capacity organ chambers and bathed in Kreb's-Henseleit solution (118 mM NaCl, 4.7 mM KCl, 1.5 mM $CaCl_2$, 1.2 mM $MgSO_4$, 1.2 mM KH_2PO_4, 25 mM $NaHCO_3$, 11 mM glucose, and 0.002 mM EDTA, pH 7.4), which was continuously gassed with 95% O_2/5% CO_2 and maintained at 37°C. Tension was measured isometrically using a force displacement transducer (NIHON KONDEN Co., Ltd., Tokyo, Japan) and was displayed on a multipen recorder (PHOENIX, TOA Electronics Ltd., Tokyo, Japan). The Krebs-Henseleit solution was changed every 15 min during equilibration. After 1 h equilibration pe-

riod, rings were stimulated with 50 mM of KCl to confirm their viability, and the following experiments were conducted. In the studies to elucidate the effects of chronic arsenic exposure on the function of the vascular endothelium, after a plateau of submaximal tension initially induced with 0.2–1 μM phenylephrine (PE, Sigma), an α-adrenergic agonist, was attained, the rings were exposed to acetylcholine (ACh, Sigma) (1 nM to 1 μM), or a calcium ionophore A23187 (A23187, Sigma) (1 nM to 1 μM) to construct dose-response curves. All concentrations indicated for the in vitro studies are final concentrations in the tissue bath. In parallel experiments, the rings were preincubated with 200 U/ml of bovine Cu, Zn-SOD (Sigma), 10 μM BH_4 (Schircks Laborataories, Jona, Switzerland), 100 μM diphenyleneiodonium (DPI), allopurinol, indomethacin, or 1 mM of N^G-nitro-L-arginine methyl ester (L-NAME) (all from Sigma) before the addition of A23187.

Determination of BH_4 in liver

Because the quinonoid form of dihydrobiopterin (qBH_2) is quite unstable and rapidly rearranged nonenzymatically to the more stable 7,8-BH_2, the amount of BH_4 was estimated from the difference between the total (acid oxidized biopterin level = BH_4 + BH_2 + oxidized biopterin) and alkaline-stable biopterin (alkaline oxidized biopterin level = BH_2 + oxidized biopterin). Biopterin contents were determined by high performance liquid chromatography (HPLC) according to previous methods [47,48] with some modification. Briefly, livers were homogenized in 0.1 mM phosphoric acid using a polytron and centrifuged at 15,000 × *g* for 10 min. The supernatant (2 ml) was mixed with 1 nmol D-threo-biopterin (Schircks Laboratories) as an internal standard and 0.25 ml 2 N trichloroacetic acid or 2 N NaOH. The mixtures were oxidized by 0.5% I_2/1% KI in 0.2 N trichloroacetic acid or 0.2 N NaOH for 1 h in dark and then neutralized to pH 4 with NaOH or trichloroacetic acid. The neutralized sample was then applied to a column containing 1 ml strong cation-exchange resin AG50W-X8 (Bio-Rad Lab., Richmond, CA, USA), which had been equilibrated with double-distilled water (DDW). The column was washed with 5 ml of DDW and biopterin was eluted with 2 ml NH_3OH/Methanol (1:1 by volume). The elutions were dried at 75°C under N_2 gas in dark. The residues were dissolved in 0.2 ml DDW and 20 μl was used for determination. The chromatographic equipment consisted of a Shimadzu solvent delivery system (a SCL-6A system controller and two LC-6A pump), a Shimadzu Chromatopac C-R1 integrator, and a Shimadzu RF-550 spectrofluorometric detector (λ^{ex} = 350 nm, λ^{em} = 450 nm, Time constant, 1.5; sensitivity, high; Range, 1) (Kyoto, Japan). Separation was carried out with an ODS column (YMC-Pack ODS-AL, 250 × 4.6 mm I.D., S-5 μm) equipped with an ODS guard column (23 × 4 mm I.D.) by a mobile phase (methanol/10 mM Kpi [pH 7.0] = 25:975, v/v) at a flow rate of 1 ml/min.

RNA blot analysis of GTP-CH I

The RNA blot analysis of GTP-cyclohydrolase-I (GTP-CH I) was performed essentially as described by Gutlich et al. [49]. Briefly, total RNA was extracted from liver using ISOGEN. Twenty micrograms of total RNA were electrophoresed on a 1% agarose gel containing 1.8% formaldehyde. RNA samples were blot transferred to ZetaProbe membrane and UV autocross-linked. Because the cDNA sequence of rabbit GTP-CH I is still unclear, the 556-bp region of the rat GTP-CH I cDNA (Accession: M58364, J05729) that corresponds to nucleotide position +276 to +831 was amplified by RT-PCR. DNA probes were labeled with ^{32}P-dCTP (specific activity 3000 Ci/mmol, Amersham-Pharmacia Biotech, Buckinghamshire, UK) by random priming. Membranes were hybridized overnight at 42°C according to the manufacturer's protocol. The hybridized filters were washed at 55°C for 30 min in 0.1 SSC/0.1% SDS and developed by autoradiography. Relative mRNA levels were quantitated by densitometric analysis.

Determination of L-arginine and its methylated metabolites

Levels of L-arginine and its methylated metabolites in the heart ventricles were determined using a previously described method [50]. Ventricle tissues of ventricle were homogenized in cold 50 mM KH_2PO_4-Na_2HPO_4 buffer (pH 7.4) containing 1 mM EDTA, 0.2% triton X-100, 1 mM PMSF, and 1 μg/ml leupeptin and centrifuged at 10,000 × *g* for 1 h. The supernatants were extracted with a strong cation-exchange resin AG50W-X8 with L-homoarginine (Sigma) as an internal standard. After extracted samples were converted to fluorescent derivatives with *o*-phthalaldehyde (OPA, Sigma) in an alkaline medium, high-performance liquid chromatographic separation with an ODS column (YMC-Pack ODS-AP, 250 × 4.6 mm I.D., 5 μm particles, 300 Å pore diameter) was performed with an isocratic mobile phase composed of citrate buffer (50 mM, pH 6.8), methanol and acetonitrile (citrate buffer/methanol/acetonitrile = 920:72:153 by volume) at a flow rate of 1 ml/min. L-arginine and its methylated metabolites were measured fluorimetrically at excitation and emission wavelengths of 340 nm and 455 nm, respectively. Protein content was determined by the method of Bradford [51] with bovine serum albumin as a standard.

Table 1. Average Body Weight and Total Food, Water and Arsenic Intake of Rabbits During the Period of Exposure

Groups	Body weight (kg)		Total food intake (kg/rabbit)	Total water intake (l/rabbit)	Total As intake (mg/rabbit)
	Initial	Final			
C	1.52 ± 0.02	3.62 ± 0.24	18.7 ± 2.3	38.4 ± 4.5	0
As(V)	1.53 ± 0.07	3.70 ± 0.24	19.0 ± 1.8	36.3 ± 3.0	181.6 ± 14.9

C = control rabbits; As(V) = arsenate-exposed rabbits. Values shown are mean ± SD of six animals/group.

Arsenic content in biological samples

Quantification of total arsenic consisting of inorganic arsenic and its methylated metabolites in blood, urine, and hair was performed as reported previously [52]. Briefly, 0.25 g of hair or 0.5 ml of each other sample was transferred into a 10 ml polymethylpentane test tube, and after the addition of 2 ml of 2 M NaOH to the sample, the mixture was heated at 95°C for 3 h. The assay sample was stirred with a magnetic stirrer once every 30 min. The treated sample was diluted to make 10 ml, and an aliquot sample was used for each assay. Inorganic arsenic and its methylated metabolites were determined by an atomic absorption spectrophotometer (Shimadzu model AA-6103). The detection limit of the three chemical species of arsenic by this method was 1 ng, with coefficient of variation being less than 5%. The standard reference material used was oyster tissue (No. 1566) from National Institute of Standards and Technology (Washington, DC, USA).

Statistical analysis

Data are expressed as mean ± SEM in all cases. The data were analyzed using GraphPad Prism (3.0 version). Comparisons between arsenate-exposed and control rabbits were performed with a two-tailed, unpaired *t*-test or Mann-Whitney nonparametric test as appropriate. A value of $p < .05$ was considered statistically significant, and an asterisk (*) is used to indicate significant differences.

RESULTS

Animals

The body weight of the As(V)-exposed animals over the 18 week exposure was not significantly different from control animals. There were no treatment-based differences in consumption of water or chow, and final body weights were unaltered by As(V) in drinking water (Table 1). There were no overt signs of toxicity observed during the exposure period. The mean amount of arsenic ingested for each rabbit based on the volume of water was 182 mg during the 18 week period. The levels of total arsenic in blood, urine, and hair were 11.1, 38.6, and 38.9 times higher, respectively, than those in the controls (Table 2).

Table 2. Levels of Total Arsenic in Blood, Urine, and Hair of Rabbits

Group	Blood (μg/l)	Urine (μg/l)	Hair (μg/kg)
C	0.37 ± 0.04	1.21 ± 0.13	60 ± 5
As(V)	4.11 ± 0.3	46.6 ± 2.8	2220 ± 300

C = control rabbits; As = arsenate-treated rabbits. Total arsenic indicates the sum of inorganic arsenic and its monomethyl and dimethyl metabolites. Each value is the mean ± SD of six animals.

Changes in plasma levels of NO metabolites and cGMP

As shown in Fig. 1, the 18 week exposure of rabbits to As(V) in drinking water resulted in a significant 24% decrease in plasma NO metabolites (nitrite and nitrate) levels compared to controls (26.5 ± 1.3 vs. 34.7 ± 2.8 μM). This is similar to the observed decrease in NO metabolites in the serum of persons chronically exposed to high levels of inorganic arsenic that we recently observed in Wuyuan, Inner Mongolia, China [7]. Furthermore, the plasma level of cGMP, which can be increased by NO and plays an important role in vasorelaxation

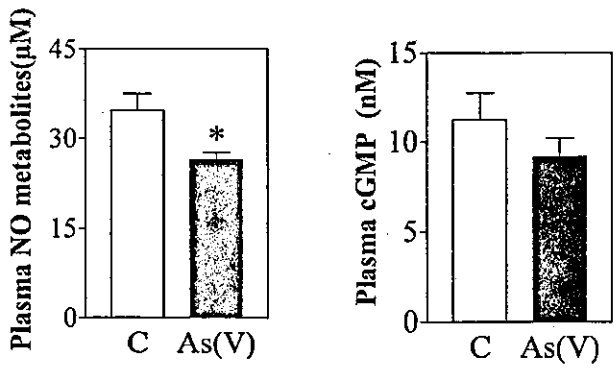

Fig. 1. Effects of prolonged arsenate exposure on plasma levels of the NO metabolites and cGMP in rabbits. Plasma levels of NO metabolites were measured as combined levels of nitrite and nitrate. C = control; As(V) = arsenate. Each data point is the mean ± SEM of three separate determinations in six animals. * $p < .05$ vs. control.

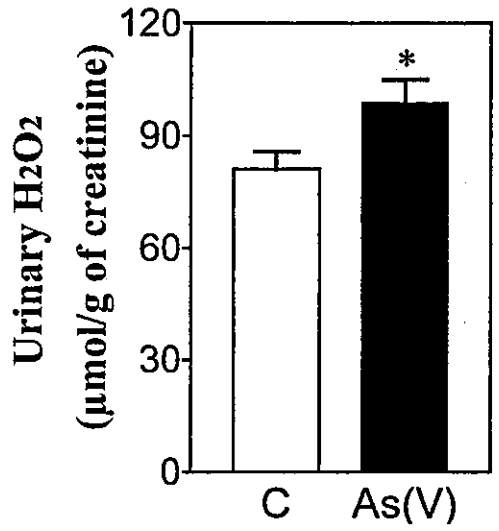

Fig. 2. H_2O_2 levels excreted in urine of rabbits after prolonged exposure to arsenate. C = control; As(V) = arsenate. Each data point is the mean ± SEM of two separate determinations in six animals. * $p < .05$ vs. control.

[51], decreased nearly 20% in As(V)-exposed rabbits (9.2 ± 0.99 nM) compared to control (11.3 ± 1.5 nM), a difference that approached statistical significance ($p = .17$).

Change in urinary H_2O_2

Since it has been reported that urinary H_2O_2 concentration is utilized as an index for oxidative stress in vivo [53,54], levels of urinary H_2O_2 were assessed after 18 weeks of As(V) exposure. As shown in Fig. 2, over 18 weeks exposure, the mean level of H_2O_2 excreted in urine of As(V)-exposed rabbits was about 1.2 times higher than that of control rabbits (99.0 ± 6.1 vs. 81.1 ± 4.7 μmol/g of creatinine), which was a significant increase.

A23187- and ACh-induced constriction in the aorta rings of the As(V)-exposed rabbits

The additions of ACh and A23187 produced dose-dependent relaxation in the aortic rings with intact aortic endothelium obtained from both As(V)-exposed and control groups. As(V) exposure did alter the endothelium-dependent maximal relaxation induced by ACh in intact thoracic aortic rings, whereas a decrease of the maximal relaxation induced by A23187 was observed (46.7% vs. 68.5%), which approached significance ($p = .09$) (Table 3). Furthermore, as shown in Fig. 3 (left), after precontraction of aortic rings with PE, the additions of A23187, which enhances intracellular calcium levels, evoked fast and transient constrictions in the aorta rings of As(V)-exposed rabbits, whereas minimal effects were observed in the aortas of the control rabbits. Similar results were observed in aortic strips derived from

Table 3. ED_{50} and Maximal Relaxation of Acetylcholine- and A23187-induced Vasorelaxation in Aortic Segments with Endothelium from Arsenate-exposed and Control Rabbits

	Control	As(V)
Acetylcholine		
ED_{50} (nmol/l)	93.3 ± 32.3	124.0 ± 32.4
Maximal relaxation (%)	79.6 ± 8.8	60.6 ± 11.7
A23187		
ED_{50} (nmol/l)	87.3 ± 26.2	116.2 ± 46.1
Maximal relaxation (%)	68.5 ± 6.8	46.7 ± 9.3#

Data are means ± SEM. n = 3–5. ED_{50} is a concentration that produces 50% of the maximal response to each drug. Maximal relaxation is expressed as a percentage of contraction induced by 3 μM of phenylephrine. # Approached significance ($p = .09$ vs. control).

As(V)-exposed rabbits when ACh was used to increase intracellular free calcium instead of A23187 (right). Furthermore, as shown in Fig. 4, preincubation of the aorta rings of As(V)-exposed rabbits with 200 U/ml of Cu, Zn-SOD attenuated the A23187-induced constrictions. A similar effect was also observed by preincubation of the rings with 10 μM BH_4. Pretreatment of the rings with 100 μM DPI, which inhibits flavin-containing enzymes, including NADPH oxidase and NOS, and L-NAME, a NOS inhibitor, also diminish the constrictions induced by the calcium ionophore. Allopurinol, an inhibitor of xanthine oxidase, and indomethacin, inhibitor of cyclooxygenase, were without effect on the calcium-dependent vasoconstriction of aortic ring from As(V)-exposed rabbits (data not shown).

Changes of levels of hepatic 6-BH_4 and L-arginine in ventricle of heart

Because of limited volume of samples and low sensitivity of detection, we were unable to determine BH_4 levels in the vascular tissues, such as aortas. As shown in Fig. 5, however, hepatic BH_4 levels in As(V)-exposed rabbits significantly decreased to 62% of control (1.11 ± 0.12 vs. 1.78 ± 0.11 nmol/g of tissue). However, mRNA level of GTP-CH I gene, a rate-limiting enzyme for BH_4 biosynthesis was not decreased by As(V) exposure (Fig. 6), suggesting that the decreased levels of BH_4 that were caused by prolonged exposure to As(V) were not due to downregulation of the GTP-CH I gene. In addition, chronic As(V) exposure did not affect the levels of L-arginine in ventricle of rabbit hearts (5.13 ± 0.91 vs. 5.41 ± 0.87 μmol/g of protein). In the determination of L-arginine in ventricle of rabbit hearts by HPLC, little L-NMMA and ADMA peaks were detected in ventricle samples of both groups (data not shown).

DISCUSSION

Present study indicates that 18 weeks of oral exposure to As(V) in rabbits resulted in a significant decrease in

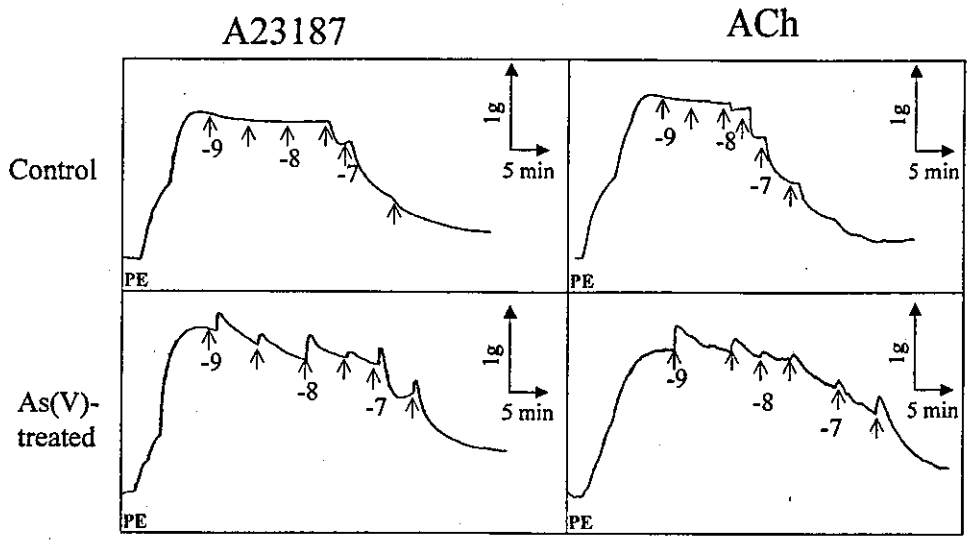

Fig. 3. Representative tracings of calcium ionophore A23187 and ACh induced relaxation and constriction in phenylephrine precontracted thoracic aortas with intact endothelium of arsenate exposed rabbits and controls. PE = phenylephrine; tracings are typical of three to five separate observations. Arrows on the traces indicate the additions of A23187 or ACh. Figures under the arrows are the final concentrations of A23187 or ACh expressed as log molar units.

plasma NO metabolites levels and a significant increase in the urinary H_2O_2 level. These observations strongly suggest that exposure to inorganic arsenate in the drinking water can reduce systemic NO production and potentially increase oxidative stress in an animal model system that metabolizes inorganic arsenic in a fashion similar to humans [42]. In this regard, reduced systemic NO production and inductions of oxidative stress have been observed in an area of endemic chronic arsenic poisoning in Inner Mongolia, China, where more than 80% of the arsenic in drinking water was in the form of inorganic As(V) [7,26]. It should be noted that because rabbits, like humans, metabolize inorganic arsenic to methylated products [42], it is possible that some of the effects on NO metabolism seen in As(V)-treated rabbits could be caused by the arsenical containing metabolites. Denninger and Marletta [55] reported that eNOS is capable of producing abundant NO and minimal $O_2^{\bullet -}$ from L-arginine under normal conditions, but this reaction requires a variety of cofactors such as NADPH, calmod-

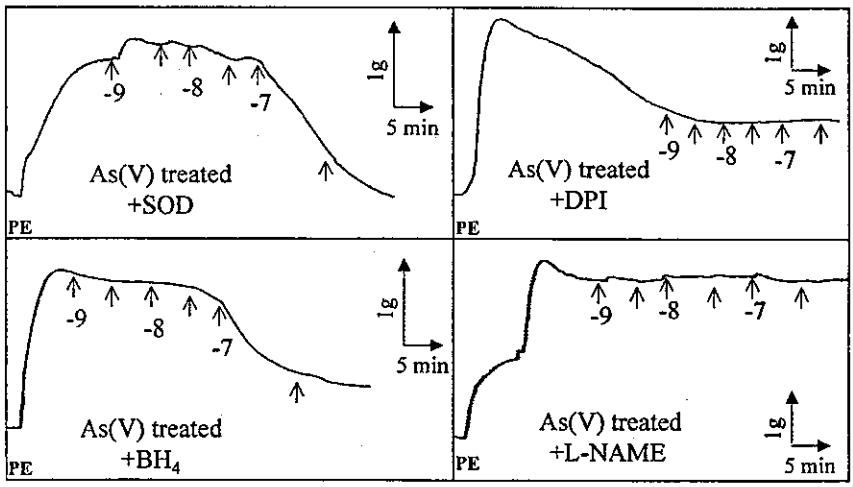

Fig. 4. Effects of SOD, BH_4, DPI, and L-NAME on the vasoconstrictions of thoracic aortas with intact endothelium of arsenate-exposed rabbits induced by A23187. PE = phenylephrine; SOD = Cu,Zn-superoxide dismutase; DPI = diphenyleneiodonium; L-NAME = N^G-nitro-L-arginine methyl ester. Tracings are typical of two to four separate observations. Arrows on the traces indicate the additions of A23187 and figures under the arrows on the traces are the concentrations of A23187 expressed as log molar units.